Bulletin of Biomathematics, 2023, 1(1), 78–110
https://www.bulletinbiomath.org
ISSN Online: 2980-1869 / Open Access
https://doi.org/10.59292/bulletinbiomath.2023005

RESEARCH PAPER

A fractional order vaccination model for COVID-19 incorporating environmental transmission: a case study using Nigerian data

Anne Ojoma Atede [1,*,‡], **Andrew Omame** [1,2,‡] **and Simeon Chioma Inyama** [1,‡]

[1]Department of Mathematics, Federal University of Technology, Owerri, Nigeria, [2]Abdus Salam School of Mathematical Sciences, Government College University Katchery Road, Lahore 54000, Pakistan

[*] Corresponding Author
[‡] anoja4god@gmail.com (Anne Ojoma Atede); andrew.omame@futo.edu.ng (Andrew Omame); scinyamam2011@yahoo.com (Simeon Chioma Inyama)

Abstract

In this work, a fractional-order vaccination model for the novel Coronavirus 2019 (COVID-19) incorporating environmental transmission is considered and analyzed using tools of fractional calculus. The Laplace transform technique and the fixed point theorem lay out the model solutions' existence and uniqueness. The solutions' positivity and boundedness are also demonstrated. Additionally, the stability of the model's equilibrium points is discussed using the fractional-order system stability theory. The model is fitted using the data sets for the Pfizer vaccination program in Nigeria from April 1, 2021, to June 10, 2021. In conclusion, simulation results for various fractional parameter values are presented. It has been observed that increasing fractional-order values has distinct effects on the various model compartments, for $\mathcal{R}_0 < 1$ and $\mathcal{R}_0 > 1$, respectively.

Keywords: Fractional derivative; stability; COVID-19; environmental transmission; numerical simulation

AMS 2020 Classification: 34C60; 92C42; 92D30; 92D25

1 Introduction

In 1965, scientists found a human coronavirus in the passageway that separates the upper and lower parts of the human body to let in and let out the air. [1] was the first discovered in an adult with a common cold. Humans can become infected with seven different kinds of coronavirus. In 2002, the sort liable for the serious intense respiratory condition (SARS) arose in South China. For a brief period, it impacted 28 different nations, giving an all-out number of around 8000

➤ **Received:** 28.03.2023 ➤ **Revised:** 25.04.2023 ➤ **Accepted:** 28.04.2023 ➤ **Published:** 30.04.2023

additional infected individuals bringing about 774 passings by July 2003, with a little increase in 2004 having just four additional cases, [2]. Experts believe that bats are the source of the coronavirus (SARS-COV2), which also gave rise to the middle east respiratory syndrome (MERS) and severe acute respiratory syndrome (SARS) [3]. It is one of a group of viruses that can cause a variety of symptoms, including fever, pneumonia, difficulty breathing, and a lung infection. In China, Wuhan Hubei province, an outbreak of a respiratory illness occurred in December 2019. The WHO declared Coronavirus disease (COVID-19) a global public health emergency due to the virus's rapid spread and as the leading cause of this illness. According to WHO, it affected roughly 19 countries by the end of January 2020, with 11791 confirmed cases and 213 deaths. The common symptoms are dry cough, exhaustion, fever (although some older people may not experience these symptoms), aches and pains, nasal congestion, a runny nose, sore throat, or diarrhea [4]. Droplets from the infected person's mouth or nose can spread the virus between people who are within two meters away from each other. It can likewise be spread in ineffectively ventilated indoor settings where individuals stay for a more broadened period, [4]. Reports show that transmission in children between the ages of 10-14 and teenagers have lower vulnerability than grown-ups, [5], [6]. Millions of people around the world, including in China, Canada, the United States, France, and Germany, have contracted COVID-19 since its discovery. According to the National Centers for Disease Control and Prevention (NCDC), as of June 25, 2021, approximately 167430 individuals in Nigeria had been identified as carrying the virus, 163937 individuals had been discharged, and approximately 2119 deaths had been recorded [7].

Mathematical models have become excellent tools for comprehending the behavior of infectious diseases [8, 9]. There have been a variety of approaches taken to investigate the means by which the disease is transmitted from person to person, the ways in which it can be avoided, and the possibilities for infectious disease control. Mathematical models have been an essential device or tool in completing this task. Numerous models have been developed by numerous individuals, including mathematicians and biologists, since the COVID-19 outbreak to explain the virus's spread from person to person. Mathematical modeling of COVID-19 transmission was taken into consideration by Sarita et al. [10]. They considered the roles of different intervention strategies such as lockdown, quarantine, and isolation of symptomatic individuals. They concluded in the model's numerical simulation and sensitivity analysis that disease could be prevented or controlled by minimizing close association, increasing the effectiveness of confined and quarantined individuals with symptoms. Enahoro et al. [11] examined the COVID-19 pandemic in Nigeria through mathematical modeling and analysis. They examined the model by applying the data gotten from the Nigeria Center for disease control (NCDC). Okuonghae and co-authors [12] analyzed Lagos' COVID-19 population dynamics using a mathematical model and concluded that the virus's prevalence would significantly decrease if regular social isolation, mask use, and other preventative measures were maintained. Bashir et al. [13] fostered an ideal optimal control model for the Coronavirus (COVID-19) pandemic. Their findings demonstrated that the control effect of increasing the number of susceptible individuals decreases the number of infectious individuals. Mohammed and others [14] looked into a fractional-order mathematical model for the dynamics of COVID-19 that included quarantine, isolation, and the viral load in the environment. The model's numerical simulation demonstrated that a 50% increase in the isolation rate of exposed individuals will significantly reduce the number of infected cases. It would likewise be diminished if the asymptomatic infected individual could take precautionary measures and quit working uninhibitedly in a susceptible population. Omame et al. [9] developed a fractional-order model for COVID-19 and tuberculosis co-infection utilizing the Atangana-Baleanu derivative. According to their simulations, reducing the risk of COVID-19 infection among people with inactive tuberculosis also reduces the spread of the virus and the two diseases simultaneously affecting a population. Using the Caputo-Fabrizio derivative and the homotopy analysis transform, Baleanu et al. examined a fractional-order model for COVID-19 transmission in their research. A convergent series solution was provided for the model [16]. Rezapour and others [15] also considered a Caputo derivative-based SIR model; using reliable data and an approximate fractional Euler solution, their model predicts the transmission of COVID-19 from one infected person to another in Iran and around the world.

Fractional differential equations have gained wider applications in the modelling of physical and biological processes in recent years [17–20]. It has demonstrated its importance due to its capacity to capture the memory, hereditary, and also properties that are not local [21]. Fractional derivatives and integrals are crucial for epidemiological modeling as they store relevant information for recollection, which will assist with spreading disease. A lot of models to control disease circulation have been extensively analyzed using fractional derivatives [22–26].

With the help of the Caputo fractional-order derivative, the primary goal of this study will be to develop a novel vaccination model for COVID-19 that incorporates environmental transmission and is tailored to actual Nigerian data. This study will significantly contribute to understanding the effective transmission of Coronavirus in our immediate environment. The main motivation for using the Caputo fractional derivative is that it has a unique way of dealing with pressing issues that affect people, like an epidemic, and also allows the conventional, initial, and boundary conditions to be taken into account [27, 28].

2 Preliminaries

Some relevant definitions and methodologies required in this paper are now highlighted in this subsection.

Definition 1 *[29] Fractional integral of order $\psi > 0$, $\psi \in \mathbb{R}^+$ reads*

$$J_t^{\psi} f(t) = \frac{1}{\Gamma(\psi)} \int_0^t (t-\zeta)^{\psi-1} f(\zeta) d\zeta, \qquad t > 0,$$

with the symbol Γ as the Gamma function given as

$$\Gamma(\psi) = \int_0^{\infty} \exp(-\zeta)\zeta^{\psi-1} d\zeta, \quad \Gamma(\psi+1) = \psi\Gamma(\psi), \quad Re\{\psi\} > 0,$$

where $f(t) = 1$, the fractional integral of order $\psi > 0$ reads

$$J_t^{\psi}(1) = \frac{1}{\Gamma(\psi)} \int_0^t (t-\zeta)^{\zeta-1}(1) d\zeta = \frac{t^{\psi}}{\Gamma(\psi+1)}.$$

Definition 2 *[29] Caputo fractional derivative of order $\psi > 0$, $\psi \in \mathbb{R}^+$ reads*

$$D_t^{\psi} f(t) = J_t^{n-\psi} D^n f(t) = \frac{1}{\Gamma(n-\psi)} \int_0^t (t-\zeta)^{n-\psi-1} f^{(n)}(\zeta) d\zeta,$$

having n as a non-negative integer giving as $n-1 < \psi \leq n$, and $0 < \psi \leq 1$, the definition above reduces to

$$D_t^{\psi} f(t) \;=\; \frac{1}{\Gamma(1-\psi)} \int_0^t (t-\zeta)^{-\psi} f'(\zeta) d\zeta. \tag{1}$$

Definition 3 ([29]) *Caputo fractional derivatives can simply be defined as*

$$D_t^{\psi} (t-t_0)^q = \frac{\Gamma(q+1)(t-t_0)^{q-\psi}}{\Gamma(q-\psi+1)},$$

with $0 < \psi \leq 1, q > -1$.

Definition 4 *Series expansion of the Mittag-Leffler of two-parameter* α_1, α_2 *type function is given as*

$$E_{\alpha_1,\alpha_2}(z) \;=\; \sum_{r=0}^{\infty} \frac{z^r}{\Gamma(\alpha_1 r + \alpha_2)}, \quad \alpha_1 > 0, \quad \alpha_2 > 0, \quad z \in \mathbb{C}. \tag{2}$$

It follows from (2) that

$$E_{1,1}(z) = \sum_{r=0}^{\infty} \frac{z^r}{\Gamma(r+1)} = \sum_{r=0}^{\infty} \frac{z^r}{r!} = e^z,$$

The renowned exponential function. Further

$$E_{1,2}(z) = \sum_{r=0}^{\infty} \frac{z^r}{\Gamma(r+2)} = \sum_{r=0}^{\infty} \frac{z^r}{(r+1)!} = \frac{1}{z} \sum_{r=0}^{\infty} \frac{z^{r+1}}{(r+1)!} = \frac{e^z - 1}{z},$$

Generally

$$E_{1,n}(z) = \frac{1}{z^{n-1}} \times \left(e^z - \sum_{r=0}^{n-2} \frac{z^r}{\Gamma(r+1)} \right).$$

Definition 5 *[29] Laplace transform of Caputo fractional derivative (1) is given as*

$$\mathcal{L}\left\{ D_t^{\psi} f(t) \right\} \;=\; s^{\psi} \tilde{f}(s) - s^{\psi-1} f(0), \quad 0 < \psi \leq 1, \tag{3}$$

with $\mathcal{L}$ as the Laplace transform operator, and $\tilde{f}(s) = \mathcal{L}\{f(t)\}$.

Lemma 1 *[30] Given* $\psi \in \mathbb{R}^+$, $\theta_1(t)$ *and* $\theta_2(t)$ *stand for the non-negative functions and* $\theta_3(t)$ *stands for both the non-negative together with the increasing function for* $0 \leq t \leq S$, $S > 0$, $\theta_3(t) \leq N$, *with* N *as a* *constant. Supposing*

$$\theta_1 \leq \theta_2 + \theta_3(t)\int_0^t (t-\zeta)^{\psi-1}\theta_1(\zeta)d\zeta,$$

then

$$\theta_1 \leq \theta_2 E_\psi\left(\theta_3(t)\frac{\pi}{\Gamma(1-\psi)\sin(\pi\psi)}S^\psi\right).$$

3 Model formulation

At a certain time t, we represent the entire population of humans with $N_H(t)$, which we divide into the states of being such that the occurrence of any one implies the non-occurrence of all the others (mutually exclusive) subdivision of a population of unvaccinated susceptible individuals $(S_{\text{c}}(t))$, individuals vaccinated with the *Pfizer* vaccine $(V_{\text{c}}(t))$, asymptomatic infectious individuals $(A_{\text{c}}(t))$, unvaccinated symptomatic infectious individuals $(J_{\text{U}}(t))$, vaccinated symptomatic infectious individuals $(J_{\text{V}}(t))$ and recovered individuals $(R(t))$. Hence, $N_{\text{H}}(t) = S_{\text{c}} + V_{\text{c}} + A_{\text{c}} + J_{\text{U}} + J_{\text{V}} + R$.

How do we get the population of unvaccinated susceptible individuals, S_{c}, created by bringing in new individuals at the rate Ω. Contacts with an infected environment cause individuals to be infected with COVID-19 and therefore reduce an entire population at the rate ϑC_{EV} and contacts with infected individuals at the rate: $\frac{\beta(\omega A_{\text{C}}+I_{\text{U}}+\varrho_{\text{V}} I_{\text{V}})}{N_{\text{H}}}$. The modification parameter $0 < \theta < 1$, accounts for reduced probability of transmission by asymptomatic infectious individuals. The parameter $\varrho_{\text{V}}(\varrho_{\text{V}} < 1)$ is a modification term accounting for the reduced infectiousness of vaccinated infectious individuals. β is the effective contact rate for transmitting COVID-19 infection from humans. ϑ is the effective contact rate for the transmission of COVID-19 infection from the infected environment. C_{EV} is the concentration of COVID-19 in the environment. We can define the active changing mode by which the fractional order model for COVID-19 is being transmitted in a population by the system of non-linear fractional differential equations in Eq. (4) below, alongside the Table 1 depicting the connected state variables and parameters in the model (4).

$$\begin{aligned}
D_t^\psi S_{\text{c}} &= \Omega - \delta S_{\text{c}} - \left(\frac{\beta(\omega A_{\text{c}} + J_{\text{U}} + \varrho_{\text{V}} J_{\text{V}})}{N_{\text{H}}}\right) S_{\text{c}} - \vartheta C_{\text{EV}} S_{\text{c}} - \mu S_{\text{c}}, \\
D_t^\psi V_{\text{c}} &= \delta S_{\text{c}} - (1-\xi)\left(\frac{\beta(\omega A_{\text{c}} + J_{\text{U}} + \varrho_{\text{V}} J_{\text{V}})}{N_{\text{H}}} + \vartheta C_{ev}\right) V_{\text{c}} - \mu V_{\text{c}}, \\
D_t^\psi A_{\text{c}} &= p\left(\frac{\beta(\omega A_{\text{c}} + J_{\text{U}} + \varrho_{\text{V}} J_{\text{V}})}{N_{\text{H}}} + \vartheta C_{\text{EV}}\right) S_{\text{c}} + f(1-\xi)\left(\frac{\beta(\omega A_{\text{c}} + J_{\text{U}} + \varrho_{\text{V}} J_{\text{V}})}{N_{\text{H}}} + \vartheta C_{\text{EV}}\right) V_{\text{c}} \\
&\quad -(\gamma_{\text{A}} + \mu) A_{\text{c}}, \\
D_t^\psi J_{\text{U}} &= (1-p)\left(\frac{\beta(\omega A_{\text{c}} + J_{\text{U}} + \varrho_{\text{V}} J_{\text{V}})}{N_{\text{H}}} + \vartheta C_{\text{EV}}\right) S_{\text{c}} - (\gamma_{\text{JU}} + d_{\text{JU}} + \mu) J_{\text{U}}, \\
D_t^\psi J_{\text{V}} &= (1-f)(1-\xi)\left(\frac{\beta(\omega A_{\text{c}} + J_{\text{U}} + \varrho_{\text{V}} J_{\text{V}})}{N_{\text{H}}} + \vartheta C_{\text{EV}}\right) V_{\text{c}} - (\gamma_{\text{JV}} + d_{\text{JV}} + \mu) J_{\text{V}}, \\
D_t^\psi R &= \gamma_{\text{A}} A_{\text{c}} + \gamma_{\text{JU}} J_{\text{U}} + \gamma_{\text{JV}} J_{\text{V}} - \mu R, \\
D_t^\psi C_{\text{EV}} &= \chi_1 A_{\text{c}} + \chi_2 J_{\text{U}} + \chi_3 J_{\text{V}} - \mu_{\text{EV}} C_{\text{EV}},
\end{aligned} \tag{4}$$

with the corresponding initial conditions

$$S_{C}(0) \geq 0, V_{C}(0) \geq 0, A_{C}(0) \geq 0, J_{U}(0) \geq 0, J_{V}(0) \geq 0, R(0) \geq 0, C_{EV}(0) \geq 0. \quad (5)$$

Table 1. Representation of the variables in the model (4)

Variable	Interpretation
S_c	unvaccinated susceptible individuals
V_c	Vaccinated with vaccine (*Pfizer*)
A_c	Asymptomatic individuals (vaccinated and unvaccinated)
J_u	unvaccinated symptomatic individuals
J_v	Vaccinated symptomatic individuals
R	Recovered humans
C_{ev}	COVID-19 concentration in the environment

Table 2. Representation of parameters in the model (4)

Parameter	Interpretation	Baseline Value	Reference
Ω	Recruitment rate	$\frac{206139587}{54.69\times 365} day^{-}1$	[31]
β	Effective transmission rate of COVID-19	0.00016708	Fitted
δ	COVID-19 vaccination rate	$0.0059 day^{-}1$	Fitted
μ	Natural death rate	$\frac{1}{54.69\times 365} day^{-}1$	[31]
ξ	COVID-19 vaccine efficacy	0.95	[32]
p	Fraction of unvaccinated susceptible that move to asymptomatic class	0.5	Assumed
f	Fraction of vaccinated susceptible that move to asymptomatic class	0.5	Assumed
ω	Modification parameter that accounts for reduced infectiousness of humans in J_u class in comparison with humans in J_v class	0.7	[12]
$\gamma_a, \gamma_{ju}, \gamma_{jv}$	Recovery rates for individuals in the A_c, J_u, and J_v classes, respectively	$0.13978 day^{-}1$	[12]
μ_{ev}	COVID-19 removal rate from the environment	$0.03 day^{-}1$	Assumed
d_{ju}, d_{jv}	Disease induced death rates for individuals in the J_u, and J_v classes, respectively	0.015	[12]
χ_1, χ_2, χ_3	Virus shedding rates from infected humans	$0.0005 day^{-}1$	Assumed

Fundamentals of the model

The boundedness and positivity of the solutions prove that equations (4)-(5) are mathematically and biologically presented.

Invariant domain

Theorem 1 *Assume $S_{\text{c}}(t)$, $V_{\text{c}}(t)$, $A_{\text{c}}(t)$, $J_{\text{U}}(t)$, $J_{\text{V}}(t)$, $R(t)$, $C_{\text{EV}}(t)$, are solutions to the equations (4)-(5), then*

i. the set $\nabla = \nabla_{\text{H}} \cup \nabla_{\text{EV}}$, where,

$$\nabla_{\text{H}} = \left\{ (S_{\text{c}}(t), V_{\text{c}}(t), A_{\text{c}}(t), J_{\text{U}}(t), J_{\text{V}}(t), R(t)) \in \mathbb{R}^7_+ : S_{\text{c}} + V_{\text{c}} + A_{\text{c}} + J_{\text{U}} + J_{\text{V}} + R, \leq \frac{\Omega}{\mu} \right\},$$

$$\nabla_{\text{EV}} = \left\{ C_{\text{EV}} : C_{\text{EV}} \leq \frac{(\chi_1 + \chi_2 + \chi_3)\beta}{\mu_{\text{EV}}} \right\},$$

is positively invariant with regard to the governing model,

ii. each solution to the equations (4)-(5) beginning from the initial point S_0, E_0, I_0, R_0 and P_0 remain positive at every value of $t \geq 0$.

Proof Let us closely observe the expression below for time t

$$N_{\text{H}} = S_{\text{c}} + V_{\text{c}} + A_{\text{c}} + J_{\text{U}} + J_{\text{V}} + R. \tag{6}$$

summing up the equations corresponding to the human compartments of the model generates

$$\begin{aligned} D_t^{\psi} N_{\text{H}}(t) &= D_t^{\psi} S_{\text{c}}(t) + D_t^{\psi} V_{\text{c}}(t) + D_t^{\psi} A_{\text{c}}(t) + D_t^{\psi} J_{\text{U}}(t) + D_t^{\psi} J_{\text{V}} + D_t^{\psi} R \\ &= \Omega - (S_{\text{c}} + V_{\text{c}} + A_{\text{c}} + J_{\text{U}} + J_{\text{V}} + R)\,\mu \\ &\leq \Omega - \mu N_{\text{H}}. \end{aligned}$$

Hence, by using Laplace transform, the inequality becomes

$$s^{\psi} \tilde{N}_{\text{H}}(s) - s^{\psi-1} N_{\text{H}}(0) \leq \frac{\Omega}{s} - \mu \tilde{N}_{\text{H}}(s),$$

from which

$$\tilde{N}_{\text{H}}(s) \leq \frac{\Omega}{s(s^{\psi} + \mu)} + N_{\text{H}}(0) \frac{s^{\psi-1}}{s^{\psi} + \mu}.$$

By partial fraction, the above expression can be re-written as

$$\begin{aligned} \tilde{N}_{\text{H}}(s) &\leq \frac{\Omega}{\mu} \left(\frac{1}{s} - \frac{s^{\psi-1}}{\mu \left(\frac{s^{\psi}}{\mu} + 1 \right)} \right) + N_{\text{H}}(0) \frac{s^{\psi-1}}{s^{\psi} + \mu} \\ &= \frac{\Omega}{\mu} \left(\frac{1}{s} \right) - \left(\frac{\Omega}{\mu} - N_{\text{H}}(0) \right) \frac{1}{s} \left(1 + \frac{\mu}{s^{\psi}} \right)^{-1}, \\ \tilde{N}_{\text{H}}(s) &\leq \frac{\Omega}{\mu} \left(\frac{1}{s} \right) - \left(\frac{\Omega}{\mu} - N_{\text{H}}(0) \right) \sum_{r=0}^{\infty} \frac{(-\mu)^r}{s^{\psi r + 1}}. \end{aligned}$$

The inverse Laplace transform with the help of (2) gives

$$\begin{aligned} N_{\mathrm{H}}(t) &\leq \frac{\Omega}{\mu} - \left(\frac{\Omega}{\mu} - N_{\mathrm{H}}(0)\right) \sum_{r=0}^{\infty} \frac{(-\mu t^{\psi})^r}{\Gamma(\psi r + 1)} \\ &\leq \frac{\Omega}{\mu} - \left(\frac{\Omega}{\mu} - N_{\mathrm{H}}(0)\right) E_{\psi}\left(-\mu t^{\psi}\right). \end{aligned}$$

It follows that as $t \to \infty$

$$0 \leq N_{\mathrm{H}} \leq \frac{\Omega}{\mu}, \tag{7}$$

of which the requirements that make equations (4)-(5) bounded and also indicate that there is an achievable possible region. ■

Positivity

Suppose that by contradiction, the third equation of the model is not true.
Let $t_1 = \min\{t : S_{\mathrm{c}}(t)V_{\mathrm{c}}(t)A_{\mathrm{c}}(t)J_{\mathrm{U}}(t)J_{\mathrm{V}}(t)R(t)C_{\mathrm{EV}}(t) = 0\}$. Suppose $A_{\mathrm{c}}(t_1) = 0$, it suggest that $S_{\mathrm{c}}(t) > 0$, $V_{\mathrm{c}}(t) > 0$, $A_{\mathrm{c}}(t) > 0$, $J_{\mathrm{U}}(t) > 0$, $J_{\mathrm{V}}(t) > 0$, $R(t) > 0$, $C_{\mathrm{EV}}(t) > 0$, for all $[0, t_1]$, suppose by assumption, the expression below exists,

$$\begin{aligned} \Theta_1 = & \min_{0 \leq t \leq t_1} \\ & \left\{ P\left(\frac{\beta(\omega A_{\mathrm{c}} + J_{\mathrm{U}} + \varrho_{\mathrm{V}} J_{\mathrm{V}}) + \vartheta C_{\mathrm{EV}}}{A_{\mathrm{c}}}\right) S_{\mathrm{c}} + f(1-\xi)\left(\frac{\beta(\omega A_{\mathrm{c}} + J_{\mathrm{U}} + \varrho_{\mathrm{V}} J_{\mathrm{V}}) + \vartheta C_{\mathrm{EV}}}{A_{\mathrm{c}}}\right) V_{\mathrm{c}} - (\gamma_{\mathrm{A}} + \mu) \right\}. \end{aligned}$$

It follows that

$$D_t^{\psi} A_{\mathrm{c}}(t) - \Theta_1 A_{\mathrm{c}}(t) > 0. \tag{8}$$

We state (without proof) that continuous function Φ_1 can be established in a way that the equation below is discovered

$$D_t^{\psi} A_{\mathrm{c}}(t) - \Theta_1 A_{\mathrm{c}}(t) = -\Phi_1(t).$$

With the Laplace transform, the last equality becomes

$$s^{\psi} \tilde{A}_{\mathrm{c}}(s_{\mathrm{c}}) - s^{\psi-1} A_{\mathrm{c}}(0) - \Theta_1 \tilde{A}_{\mathrm{c}}(s) = -\tilde{\Phi}_1(s),$$

from which

$$\begin{aligned} \tilde{A}_{\mathrm{c}}(s) &= A_{\mathrm{c}}(0) \frac{s^{\psi-1}}{s^{\psi} - \Theta_1} - \frac{\Phi_1(s)}{s^{\psi} - \Theta_1} = \frac{A_{\mathrm{c}}(0)}{s}\left(1 - \frac{\Theta_1}{s^{\psi}}\right)^{-1} - \frac{\Phi_1(s)}{s^{\psi}}\left(1 - \frac{\Theta_1}{s^{\psi}}\right)^{-1} \\ &= A_{\mathrm{c}}(0) \sum_{r=0}^{\infty} \frac{\Theta_1^r}{s^{\psi r + 1}} - \Phi_1(s) \sum_{r=0}^{\infty} \frac{\Theta_1^r}{s^{\psi r + \psi}}. \end{aligned}$$

The inverse Laplace transform using the Mittag-Leffler function and forgetting the non-positive term produces a solution to the above terms in (8) that meets the expression below.

$$A_{\text{c}}(t) \quad > \quad A_{\text{c}}(0)\sum_{r=0}^{\infty}\frac{(\Theta_1 t^{\psi})^r}{\Gamma(\psi r+1)} = A_{\text{c}}(0)E_{\psi}\left(\Theta_1 t^{\psi}\right).$$

Hence, the positivity of the solution A_{c} is as follows:

$$A_{\text{c}}(t) > A_{\text{c}}(0)E_{\psi}\left(\Theta_1 t^{\psi}\right) > 0,$$

which contradicts $A_{\text{c}}(t_1) = 0$. Similarly, suppose $J_{\text{U}}(t_1) = 0$ which implies that $S_{\text{c}}(t) > 0$, $V_{\text{c}}(t) > 0$, $A_{\text{c}}(t) > 0$, $J_{\text{v}}(t) > 0$, $R(t) > 0$, $C_{\text{EV}} > 0$, for all $0 \le t \le t_1$. Assume the expression is true

$$\Theta_2 \quad = \quad \min_{0\le t\le t_t}\left\{(1-p)\left(\frac{\beta(\omega A_{\text{c}} + J_{\text{U}} + \varrho_{\text{V}} J_{\text{V}}) + \vartheta C_{\text{V}}}{J_{\text{U}}}\right) S_{\text{C}} - (\gamma_{\text{JU}} + d_{\text{JU}} + \mu)\right\},$$

then

$$D_t^{\psi} J_{\text{U}}(t) \quad > \quad \Theta_2 J_{\text{U}}(t). \tag{9}$$

It follows that a continuous function $\Phi_2(t)$ may be established in a way that the equation below is discovered

$$D_t^{\psi} J_{\text{U}}(t) - \Theta_2 J_{\text{U}}(t) \quad = \quad -\Phi_2(t).$$

With the Laplace transform, the equation becomes

$$s^{\psi}\tilde{J}_{\text{U}}(s) - s^{\psi-1}J_{\text{U}}(0) - \Theta_2\tilde{J}_{\text{U}}(s) = -\tilde{\Phi}_2(s),$$

from which

$$\tilde{J}_{\text{U}}(s) \quad = \quad J_{\text{U}}(0)\frac{s^{\psi-1}}{s^{\psi}-\Theta_2} - \frac{\Phi_2(s)}{s^{\psi}-\Theta_2} = J_{\text{U}}(0)\sum_{r=0}^{\infty}\frac{\Theta_2^r}{s^{\psi r+1}} - \Phi_2(s)\sum_{r=0}^{\infty}\frac{\Theta_2^r}{s^{\psi r+\psi}}.$$

Using the inverse Laplace transform, applying the Mittag-Leffler function, and forgetting the non-positive term, the solution to the equation (9) meets that of the quantity below

$$J_{\text{U}}(t) \quad > \quad J_{\text{U}}0)\sum_{r=0}^{\infty}\frac{(\Theta_2 t^{\psi})^r}{\Gamma(\psi r+1)} = J_{\text{U}}(0)E_{\psi}\left(\Theta_2 t^{\psi}\right).$$

Hence, the positivity of the solution I_{U} is as follows

$$J_{\text{U}}(t) > J_{\text{U}}(0)E_{\psi}\left(\Theta_2 t^{\psi}\right) > 0,$$

which contradicts $J_{\text{U}}(t_1) = 0$. Applying the similar method of solution to the question above, we assume $J_{\text{v}}(t_1) = 0$ which suggests that $S_{\text{c}}(t) > 0$, $V_{\text{c}}(t) > 0$, $A_{\text{c}}(t) > 0$, J_{U}, $R(t) > 0$, $C_{\text{EV}}(t) > 0$ for all $0 \leq t \leq t_1$. Suppose the expression below is true

$$\Theta_3 = \min_{0 \leq t \leq t_t} \left\{ (1-f)(1-\xi) \left(\frac{\beta(\omega A_c + J_u + \varrho_v J_v)}{J_v} + \vartheta C_{EV} \right) V_c - (\gamma_{JV} + d_{JV} + \mu) \right\}.$$

So that

$$D_t^{\psi} J_v(t) > \Theta_3 J_v(t). \tag{10}$$

It follows that a continuous function $\Phi_3(t)$ can be established in a way that the equation below is discovered

$$D_t^{\psi} J_v(t) - \Theta_3 J_v(t) = -\Phi_3(t).$$

By using the Laplace transform, the above inequality becomes

$$s^{\psi} \tilde{J}_v(s) - s^{\psi-1} J_v(0) - \Theta_3 \tilde{J}_v(s) = -\tilde{\Phi}_3(s),$$

from which

$$\tilde{J}_v(s) = J_v(0) \sum_{r=0}^{\infty} \frac{\Theta_3^r}{s^{\psi r+1}} - \Phi_3(s) \sum_{r=0}^{\infty} \frac{\Theta_3^r}{s^{\psi r+\psi}}.$$

Applying the inverse Laplace transform using the Mittag-Leffler function and forgetting the non-positive term, the solution to the equation (10) meets that of the expression below.

$$J_v(t) > J_v(0) \sum_{r=0}^{\infty} \frac{(\Theta_3 t^{\psi})^r}{\Gamma(\psi r+1)} = J_v(0) E_{\psi} \left(\Theta_3 t^{\psi} \right). \tag{11}$$

Hence, the positivity of the solution J_v is as follows

$$J_v(t) > J_v(0) E_{\psi} \left(\Theta_3 t^{\psi} \right) > 0,$$

which is not in agreement with the fact that $J_v(t_1) = 0$. Likewise, assuming $C_{EV}(t_1) = 0$ which suggest that $S_c(t) > 0$, $V_c(t) > 0$, $A_c(t) > 0$, $J_v(t) > 0$, $R(t) > 0$, $C_{EV} > 0$, for all $0 \leq t \leq t_1$. Supposing the expression below is true

$$\Theta_4 = \min_{0 \leq t \leq t_t} \left\{ \left(\frac{\chi_1 A_c + \chi_2 J_u + \chi_3 J_v}{C_{EV}} - \mu_{EV} \right) \right\},$$

then

$$D_t^{\psi} C_{EV}(t) > \Theta_4 C_{EV}(t). \tag{12}$$

It follows that a continuous function $\Phi_4(t)$ can be established in a way the equation below is discovered

$$D_t^{\psi} C_{\text{EV}}(t) - \Theta_4 C_{\text{EV}}(t) \;=\; -\Phi_4(t).$$

By using the Laplace transform, the inequality becomes

$$s^{\psi}\tilde{C}_{\text{EV}}(s) - s^{\psi-1}C_{\text{EV}}(0) - \Theta_4\tilde{C}_{\text{EV}}(s) = -\tilde{\Phi}_4(s),$$

from which

$$\tilde{C}_{\text{EV}}(s) \;=\; C_{\text{EV}}(0)\frac{s^{\psi-1}}{s^{\psi}-\Theta_4} - \frac{\Phi_4(s)}{s^{\psi}-\Theta_4} = C_{\text{EV}}(0)\sum_{r=0}^{\infty}\frac{\Theta_4^r}{s^{\psi r+1}} - \Phi_4(s)\sum_{r=0}^{\infty}\frac{\Theta_4^r}{s^{\psi r+\psi}}.$$

Applying the inverse Laplace transform using the Mittag-Leffler function and forgetting the non-positive term, the solution to equation (12) meets that of the quantity below.

$$C_{\text{EV}}(t) \;>\; C_{\text{EV}}0)\sum_{r=0}^{\infty}\frac{(\Theta_4 t^{\psi})^r}{\Gamma(\psi r+1)} = C_{\text{EV}}(0)E_{\psi}\left(\Theta_4 t^{\psi}\right).$$

Hence, the positivity of the solution J_{U} is as follows

$$C_{\text{EV}}(t) > C_{\text{EV}}(0)E_{\psi}\left(\Theta_4 t^{\psi}\right) > 0,$$

which contradicts $C_{\text{EV}}(t_1) = 0$. Furthermore, the same method of solution will prove that the positivity of the solutions S_{c}, V_{c}, R and C_{EV} are as follows

$$S_{\text{c}}(t) > S_{\text{c}}(0)E_{\psi}\left(\Theta_5 t^{\psi}\right) > 0, \quad V_{\text{c}}(t) > V_{\text{c}}(0)E_{\psi}\left(\Theta_6 t^{\psi}\right) > 0,$$

$$R(t) > R(0)E_{\psi}\left(\Theta_7 t^{\psi}\right) > 0, \quad C_{\text{EV}}(t) > C_{\text{EV}}(0)E_{\psi}\left(\Theta_8 t^{\psi}\right) > 0.$$

Existence and uniqueness of the solution

This section shows the proof of existence and uniqueness of the solution of fractional model (4)-(5). The same solution method in [33] is employed here using the theorem of Banach fixed point and Picard's operator. Furthermore, for existence, Schauder's fixed point theorem will be applied in which the boundedness of the solution shall be proven, too.

The use of fractional integral together with the Caputo fractional derivative model (4) of order $\psi > 0$ alongside its corresponding initial conditions (5) present the Volterra-integral equations of the second kind below as well as a solution to the fractional model.

$$
\begin{aligned}
S_{c}(t)-S_{c}(0) &= \frac{1}{\Gamma(\psi)}\int_0^t (t-\zeta)^{\psi-1}L(\zeta,S_{c}(\zeta))d\zeta,\\
V_{c}(t)-V_{c}(0) &= \frac{1}{\Gamma(\psi)}\int_0^t (t-\zeta)^{\psi-1}M(\zeta,V_{c}(\zeta))d\zeta,\\
A_{c}(t)-A_{c}(0) &= \frac{1}{\Gamma(\psi)}\int_0^t (t-\zeta)^{\psi-1}N(\zeta,A_{c}(\zeta))d\zeta,\\
J_{U}(t)-J_{U}(0) &= \frac{1}{\Gamma(\psi)}\int_0^t (t-\zeta)^{\psi-1}O(\zeta,J_{U}(\zeta))d\zeta,\\
J_{V}(t)-J_{V}(0) &= \frac{1}{\Gamma(\psi)}\int_0^t (t-\zeta)^{\psi-1}P(\zeta,J_{V}(\zeta))d\zeta,\\
R(t)-R(0) &= \frac{1}{\Gamma(\psi)}\int_0^t (t-\zeta)^{\psi-1}V(\zeta,R(\zeta))d\zeta,\\
C_{EV}(t)-C_{EV}(0) &= \frac{1}{\Gamma(\psi)}\int_0^t (t-\zeta)^{\psi-1}Z(\zeta,C_{EV}(\zeta))d\zeta.
\end{aligned}
\tag{13}
$$

The functions $(L,M,N,O,P,V,Z):[0,b]\to\mathbb{R}\times\mathbb{R}$ without proof are presumed to be continuous in such a way that the Banach space, as well as the space of all the continuous functions, are $(\mathbb{R},\|.\|)$ and $\mathbb{H}^1$([0,b]) respectively which is defined in $[0,b]\to\mathbb{R}$ formed alongside Chebyshev norm.

The next thing we want to do is to show if the continuous functions L, M, N, O P, V, and Z meet the Lipschitz conditions provided

$$
\sup_{0<t\le S}\left\|\frac{A_{C}}{N_{H}}\right\|\le\varphi_1,\quad \sup_{0<t\le S}\left\|\frac{J_{U}}{N_{H}}\right\|\le\varphi_2,\quad \sup_{0<t\le S}\left\|\frac{J_{V}}{N_{H}}\right\|\le\varphi_3,\quad \sup_{0<t\le S}\left\|\frac{C_{EV}}{N_{H}}\right\|\le\varphi_4.
$$

Thus, firstly we get

$$
\begin{aligned}
\|L(S_{c1})-L(S_{c2})\| &= \Bigg\|\Omega-\left(\delta+\frac{\beta\left(\omega A_{C}+J_{U}+\varrho_{V}J_{V}\right)}{\vartheta}C_{EV}+\mu\right)S_{c1}\\
&\quad -\left(\Omega-\left(\delta+\frac{\beta\left(\omega A_{C}+J_{U}+\varrho_{V}J_{V}\right)}{N_{H}}+\vartheta C_{EV}+\mu\right)S_{c2}\right)\Bigg\|\\
&= \Bigg\|-\frac{\beta\omega A_{C}}{N_{H}}\left(S_{c1}-S_{c2}\right)-\frac{\beta J_{U}}{N_{H}}\left(S_{c1}-S_{c2}\right)-\frac{\beta\varrho_{V}J_{V}}{N_{H}}\left(S_{c1}-S_{c2}\right)-\vartheta C_{EV}\left(S_{c1}-S_{c2}\right)\\
&\quad -\mu\left(S_{c1}-S_{c2}\right)\Bigg\|\\
&\le \beta\omega\sup_{0\le t\le S}\left\|\frac{A_{C}}{N_{H}}\right\|\|S_{c1}-S_{c2}\|+\beta\sup_{0\le t\le S}\left\|\frac{J_{U}}{N_{H}}\right\|\|S_{c1}-S_{c2}\|\\
&\quad +\vartheta\sup_{0\le t\le S}\|C_{EV}\|\|S_{c1}-S_{c2}\|+\mu\|S_{c1}-S_{c2}\|+\beta\varrho_{V}\sup_{0\le t\le S}\left\|\frac{J_{V}}{N_{H}}\right\|\|S_{c1}-S_{c2}\|\\
&\le L_L\|S_{c1}-S_{c2}\|,
\end{aligned}
\tag{14}
$$

where

$$
L_L=\left(\beta\omega\varphi_1+\beta\varphi_2+\beta\varrho_{V}\varphi_3+\vartheta C_{EV}+\mu\right)>0.
$$

Secondly,

$$\begin{aligned}
\|M(V_1)-M(V_2)\| &= \Bigg\|\delta S_{\text{C}}-(1-\xi)\left(\frac{\beta(\omega A_{\text{C}}+J_{\text{U}}+\varrho_{\text{V}}J_{\text{V}})}{N_{\text{H}}}+\vartheta C_{\text{EV}}\right)V_{c1}\\
&\quad-\left(\delta S_{\text{C}}-(1-\xi)\left(\frac{\beta(\omega A_{\text{C}}+J_{\text{U}}+\varrho_{\text{V}}J_{\text{V}})}{N_{\text{H}}}+\vartheta C_{\text{EV}}+\mu\right)V_{c2}\right)\Bigg\|\\
&= -\left(\delta S_{\text{C}}+(1-\xi)\left(\frac{\beta(\omega A_{\text{C}}+J_{\text{U}}+\varrho_{\text{V}}J_{\text{V}})}{N_{\text{H}}}+\vartheta C_{\text{EV}}+\mu\right)\right)\|V_{c1}-V_{c2}\|\\
&= \Bigg((1-\xi)\,\beta\omega\sup_{0\le t\le S}\left\|\frac{A_{\text{C}}}{N_{\text{H}}}\right\|+(1-\xi)\,\beta\sup_{0\le t\le S}\left\|\frac{J_{\text{U}}}{N_{\text{U}}}\right\| \qquad (15)\\
&\quad+(1-\xi)\,\beta\varrho_{\text{V}}\sup_{0\le t\le S}\left\|\frac{J_{\text{V}}}{N_{\text{H}}}\right\|+\delta S_{\text{C}}+\vartheta C_{\text{EV}}+\mu\Bigg)\|V_{c1}-V_{c2}\|\\
&\le L_M\|V_{c1}-V_{c2}\|,
\end{aligned}$$

where

$$L_M=((1-\xi)\,\beta\omega\varphi_5+(1-\xi)\,\beta\varphi_3+(1-\xi)\,\beta\varrho_{\text{V}}\varphi_4+\delta S+\vartheta C_{\text{EV}}+\mu)>0.$$

Applying the same method below, we get

$$\begin{aligned}
\|N(A_{c1})-N(A_{c2})\| &= \left\|\left(-(\gamma_A+\mu)\,A_{\text{C}}+P\left(\frac{\beta\,(\omega A_{\text{C}}+J_{\text{U}}+\varrho_{\text{V}}J_{\text{V}})}{N_{\text{H}}}+\vartheta_{\text{EV}}\right)S_{\text{C}}\right)\right\|\\
&\quad+\left\|f\,(1-\xi)\left(\left(\frac{\beta\,(\omega A_{\text{C}}+J_{\text{U}}+\varrho_{\text{V}}J_{\text{V}})}{N_{\text{H}}}+\vartheta C_{\text{EV}}\right)\right)A_{c1}\right\|\\
&\quad-\left\|\left(-(\gamma_A+\mu)\,A_{\text{C}}+P\left(\frac{\beta\,(\omega A_{\text{C}}+J_{\text{U}}+\varrho_{\text{V}}J_{\text{V}})}{N_{\text{H}}}+\vartheta C_{\text{EV}}\right)S_{\text{C}}\right)\right\| \qquad (16)\\
&\quad+\left\|f\,(1-\xi)\left(\left(\frac{\beta\,(\omega A_{\text{C}}+J_{\text{U}}+\varrho_{\text{V}}J_{\text{U}})}{N_{\text{H}}}+\vartheta C_{\text{EV}}\right)A_{c2}\right)\right\|\\
&= (\gamma_A+\mu)\,\|A_{c1}-A_{c2}\|\\
&\le L_N\|A_{c1}-A_{c2}\|,
\end{aligned}$$

where

$$L_N=(\gamma_A\varphi_5+\mu\varphi_3)>0.$$

$$\begin{aligned}
\|O(J_{u1})-O(J_{u2})\| &= \Bigg\|(1-P)\left(\frac{\beta\,(\omega A_{\text{C}}+J_{\text{U}}+\varrho_{\text{V}}J_{\text{V}})}{N_H}+\vartheta C_{\text{EV}}\right)S_{\text{C}}-((\gamma_{\text{JU}}+d_{\text{JU}}+\mu))\,J_{u1}\\
&\quad-(1-P)\left(\frac{\beta\,(\omega A_{\text{C}}+J_{\text{U}}+\varrho_{\text{V}}J_{\text{V}})}{N_H}+\vartheta C_{\text{EV}}\right)S_{\text{C}}-((\gamma_{\text{JU}}+d_{\text{JU}}+\mu)\,J_{u2})\Bigg\|\\
&\le L_O\|J_{u1}-J_{u2}\|, \qquad (17)
\end{aligned}$$

where

$$L_O=(\gamma J_{\text{JU}}\varphi_1+dJ_{\text{JU}}\varphi_2+\mu)>0.$$

$$\begin{aligned}
\|P(J_{v1})-P(J_{v2})\| &= \Bigg\|(1-f)(1-\xi)\left(\frac{\beta(\omega A_{C}+J_{U}+\varrho_{V}J_{V})}{N_{H}}+\vartheta C_{EV}\right)S_{C}-(\gamma_{JV}+d_{JV}+\mu)J_{v1} \\
&- (1-f)(1-\xi)\left(\frac{\beta(\omega A_{C}+J_{U}+\varrho_{V}J_{V})}{N_{H}}+\vartheta C_{EV}\right)S_{C}-((\gamma_{JV}+d_{JV}+\mu)J_{v2})\Bigg\| \\
&\leq L_{P}\|J_{v1}-J_{v2}\|, \qquad (18)
\end{aligned}$$

where

$$L_{P}=(\gamma_{JV}\varphi_{2}+d_{JV}\varphi_{3}+\mu)>0.$$

$$\begin{aligned}
\|V(R_{1})-V(R_{2})\| &= \|\gamma_{A}A+\gamma_{JU}J_{U}+\gamma_{JV}J_{V}-(\mu)R_{1}-(\gamma_{A}A+\gamma_{JU}I_{U}+\gamma_{JV}I_{V}-(\mu)R_{2})\| \\
&\leq L_{V}\|R_{1}-R_{2}\|, \qquad (19)
\end{aligned}$$

where

$$L_{V}=(\mu)>0.$$

$$\begin{aligned}
\|Z(C_{EV1})-Z(C_{EV2})\| &= \|\chi_{1}A_{C}+\chi_{2}J_{U}+\chi_{3}J_{V}-(\mu_{EV})C_{EV1}-(\chi_{1}A_{C}+\chi_{2}J_{U}+\chi_{3}J_{V}-(\mu_{EV}))C_{EV2}\| \\
&\leq Ł_{Z}\|C_{EV1}-C_{EV2}\|. \qquad (20)
\end{aligned}$$

where

$$L_{Z}=(\mu_{EV})>0.$$

Theorem 2 *If* $(L_{L},L_{M},L_{N},L_{O},L_{P},L_{V},L_{Z})\frac{\Gamma(1-\psi)\sin(\pi\psi)T^{\psi}}{\psi\pi}<1$, *it follows that the fractional model* (4)- (5) *has a unique solution on* $[0,b]$*where* $(L,M,N,O,P,V,Z):[0,b]\times\mathbb{R}\to\mathbb{R}$ *are presumed to be continuous meeting the Lipschitz condition.*

Proof Observe the mapping below $\eta:\mathbb{H}^{1}([0,b],\mathbb{R})\to\mathbb{H}^{1}([0,b],\mathbb{R})$, with a well defined η in $(L,M,N,O,P,V,Z):[0,b]\times\mathbb{R}\to\mathbb{R}$. Using (15)-(20) and for all $((S_{c1},S_{c2})$, (V_{c1},V_{c2}), (A_{c1},A_{c2}), (J_{U1},J_{U2}), (J_{V1},J_{V2}), (R_{1},R_{2}), (C_{EV1},C_{EV2}), $\in\mathbb{H}^{1}([0,b],\mathbb{R})$ and $0\leq t\leq S$ we get

$$\begin{aligned}
\|\eta(S_{c1}(t))-\eta(S_{c2}(t))\| &= \left\|S_{c}(0)+\frac{1}{\Gamma(\psi)}\int_{0}^{t}(t-\zeta)^{\psi-1}L(\zeta,S_{c1}(\zeta))\,d\zeta\right\| \\
&\quad -\left\|\left(S_{c}(0)+\frac{1}{\Gamma(\psi)}\int_{0}^{t}(t-\zeta)^{\psi-1}L(\zeta,S_{c2}(\zeta))\,d\zeta\right)\right\| \qquad (21)\\
&\leq \frac{1}{\Gamma(\psi)}\int_{0}^{t}(t-\zeta)^{\psi-1}\|L(\zeta,S_{c1}(\zeta))-L(\zeta,S_{c2}(\zeta))\|\,d\zeta \\
&\leq \frac{L_{L}}{\Gamma(\psi)}\int_{0}^{t}(t-\zeta)^{\psi-1}\|S_{c1}(\zeta)-S_{c2}(\zeta)\|\,d\zeta \\
&\leq L_{L}\left(\frac{\Gamma(1-\psi)\sin(\pi\psi)S^{\psi}}{\psi\pi}\right)\|S_{c1}-S_{c2}\|_{\mathbb{H}^{1}}.
\end{aligned}$$

Similar process yields

$$
\begin{aligned}
\|\eta(V_{c1}(t))-\eta(_{c2}(t))\| &\leq L_M\left(\frac{\Gamma(1-\psi)\sin(\pi\psi)S^{\psi}}{\psi\pi}\right)\|V_{c1}-V_{c2}\|_{\mathbb{H}^1},\\
\|\eta(A_{c1}(t))-\eta(A_{c2}(t))\| &\leq L_N\left(\frac{\Gamma(1-\psi)\sin(\pi\psi)S^{\psi}}{\psi\pi}\right)\|A_{c1}-A_{c2}\|_{\mathbb{H}^1},\\
\|\eta(J_{u1}(t))-\eta(J_{u2}(t))\| &\leq L_O\left(\frac{\Gamma(1-\psi)\sin(\pi\psi)S^{\psi}}{\psi\pi}\right)\|J_{\text{U}1}-J_{\text{U}2}\|_{\mathbb{H}^1},\\
\|\eta(J_{v1}(t))-\eta(J_{v2}(t))\| &\leq L_P\left(\frac{\Gamma(1-\psi)\sin(\pi\psi)S^{\psi}}{\psi\pi}\right)\|J_{v1}-J_{v2}\|_{\mathbb{H}^1},\\
\|\eta(R_1(t))-\eta(R_2(t))\| &\leq L_V\left(\frac{\Gamma(1-\psi)\sin(\pi\psi)S^{\psi}}{\psi\pi}\right)\|R_1-R_2\|_{\mathbb{H}^1},\\
\|\eta(C_{\text{EV}1}(t))-\eta(C_{\text{EV}2}(t))\| &\leq L_Z\left(\frac{\Gamma(1-\psi)\sin(\pi\psi)S^{\psi}}{\psi\pi}\right)\|C_{\text{EV}1}-C_{\text{EV}2}\|_{\mathbb{H}^1}.
\end{aligned}
\tag{22}
$$

The condition clearly shows that $(L_L, L_M, L_N, L_O, L_P, L_V, L_Z)\,\frac{\Gamma(1-\psi)\sin(\pi\psi)S^{\psi}}{\psi\pi} < 1$, the parameter η is a contraction mapping and application of the Banach contraction mapping principle, signifying that the parameter η has a unique fixed point in $0 \leq t \leq S$. ■

Using the theorems of Schauder's fixed point, the existence of solutions of fractional model (4)- (5) shall be considered.

Theorem 3 *Assuming that* $(L, M, N, O, P, V, Z) : [0, b] \times \mathbb{R} \to \mathbb{R}$ *are continuous and that there is a constants* $(L_{F1}, L_{G1}, L_{H1}, L_{K1}, L_{Q1}, L_{U1}, L_{W1}) > 0$
so that
$\|F(t, S_c)\| \leq L_{F1}(d + \|S_c\|)$, $\|G(t, V_c)\| \leq L_{G1}(d + \|V_c\|)$, $\|H(t, A_c)\| \leq L_{H1}(d + \|A_c\|)$,
$\|K(t, J_{\text{U}})\| \leq L_{K1}(d + \|J_{\text{U}}\|)$, $\|Q(t, J_{\text{v}})\| \leq L_{Q1}(d + \|J_{\text{v}}\|)$, $\|U(t, R)\| \leq L_{U1}(d + \|R\|)$,
$\|W(t, C_{\text{EV}})\| \leq L_{W1}(d + \|C_{\text{EV}}\|)$, *with* $0 < d \leq 1$ *as an arbitrary number, it follows that* (4)- (5) *possesses a minimum of one solution.*

Proof From (22), it is clear that the operator η is continuous. Thus let $\{S_c^{n+1}\}_\infty, \{V_c^{n+1}\}_\infty, \{A_c^{n+1}\}_\infty$, $\{J_{\text{U}}^{n+1}\}_\infty, \{J_{\text{v}}^{n+1}\}_\infty, \{R^{n+1}\}_\infty, \{C_{\text{EV}}^{n+1}\}_\infty$, be sequences so that $S_c^{n+1} \to S_c^n$, $V_c^{n+1} \to V_c^n$, $A_c^{n+1} \to A_c^n$, $J_{\text{U}}^{n+1} \to J_{\text{U}}^n$, $J_{\text{v}}^{n+1} \to J_{\text{v}}^n$, $R^{n+1} \to R^n$, $C_{\text{EV}}^{n+1} \to C_{\text{EV}}^n$, in $\mathbb{H}^1([0, b], \mathbb{R})$. Then for every $0 \leq t \leq S$ we get

$$
\begin{aligned}
\left\|\eta S_c^{n+1}(t)-\eta S_c^n(t)\right\| &= \frac{1}{\Gamma(\psi)}\left\|\int_0^t (t-\zeta)^{\psi-1} F\left(\zeta, S_c^{n+1}(\zeta)\right)d\zeta - \int_0^t (t-\zeta)^{\psi-1} F\left(\zeta, S_c^n(\zeta)\right)d\zeta\right\|,\\
&\leq \frac{1}{\Gamma(\psi)}\int_0^h (t-\zeta)^{\psi-1}\left\|F(\zeta,^{n+1}(\zeta)) - F(\zeta, S_c^n(\zeta))\right\|d\zeta,\\
&\leq \frac{L_{F1}S^{\psi}}{\Gamma(\psi+1)}\left\|S_c^{n+1}) - S_c^n\right\|,\\
&\leq L_{F1}\left(\frac{\Gamma(1-\psi)\sin(\pi\psi)S^{\psi}}{\psi\pi}\right)\left\|S_c^{n+1}-S_c^n\right\|_{\mathbb{H}^1},
\end{aligned}
\tag{23}
$$

where $\|S_c^{n+1} - S_c^n\|_{\mathbb{H}} \to 0$ as $n \to \infty$.

Following the method of solution, we have

$$
\begin{aligned}
\left\|\eta V_{\text{c}}^{n+1}(t)-\eta V_{\text{c}}^{n}(t)\right\| &\leq L_{G1}\left(\frac{\Gamma(1-\psi)\sin(\pi\psi)S^{\psi}}{\psi\pi}\right)\left\|V_{\text{c}}^{n+1}-V_{\text{c}}^{n}\right\|_{\mathbb{H}^1},\\
\left\|\eta A_{\text{c}}^{n+1}(t)-\eta A_{\text{c}}^{n}(t)\right\| &\leq L_{H1}\left(\frac{\Gamma(1-\psi)\sin(\pi\psi)S^{\psi}}{\psi\pi}\right)\left\|A_{\text{c}}^{n+1}-A_{\text{c}}^{n}\right\|_{\mathbb{H}^1},\\
\left\|\eta J_{\text{U}}^{n+1}(t)-\eta J_{\text{U}}^{n}(t)\right\| &\leq L_{K1}\left(\frac{\Gamma(1-\psi)\sin(\pi\psi)T^{\psi}}{\psi\pi}\right)\left\|J_{\text{U}}^{n+1}-J_{\text{U}}^{n}\right\|_{\mathbb{H}^1},\\
\left\|\eta J_{\text{V}}^{n+1}(t)-\eta J_{\text{V}}^{n}(t)\right\| &\leq L_{Q1}\left(\frac{\Gamma(1-\psi)\sin(\pi\psi)S^{\psi}}{\psi\pi}\right)\left\|J_{\text{V}}^{n+1}-J_{\text{V}}^{n}\right\|_{\mathbb{H}^1},\\
\left\|\eta R^{n+1}(t)-\eta R^{n}(t)\right\| &\leq L_{U1}\left(\frac{\Gamma(1-\psi)\sin(\pi\psi)S^{\psi}}{\psi\pi}\right)\left\|R^{n+1}-R^{n}\right\|_{\mathbb{H}^1},\\
\left\|\eta C_{\text{EV}}^{n+1}(t)-\eta C_{\text{EV}}^{n}(t)\right\| &\leq L_{W1}\left(\frac{\Gamma(1-\psi)\sin(\pi\psi)S^{\psi}}{\psi\pi}\right)\left\|C_{\text{EV}}^{n+1}-C_{\text{EV}}^{n}\right\|_{\mathbb{H}^1},
\end{aligned}
$$

where $\left\|V_{\text{c}}^{n+1}-V_{\text{c}}^{n}\right\|_{\mathbb{H}^1}\to 0$, $\left\|A_{\text{c}}^{n+1}-A_{\text{c}}^{n}\right\|_{\mathbb{H}*1}\to 0$, $\left\|J_{\text{U}}^{n+1}-J_{\text{U}}^{n}\right\|_{\mathbb{H}^1}\to 0$, $\left\|J_{\text{V}}^{n+1}-J_{\text{V}}^{n}\right\|_{\mathbb{H}^1}\to 0$, $\left\|R^{m+1}-R^{n}\right\|_{\mathbb{H}^1}\to 0$, $\left\|C_{\text{EV}}^{n+1}-C_{\text{EV}}^{n}\right\|_{\mathbb{H}^1}\to 0$, Hence, the operator η is continuous. ■

Next we show that the operator η is a one-to-one bounded set of $\mathbb{H}^1([0,b],\mathbb{R})$. Therefore, for every $S_{\text{c}}\in M_{Sc}$, $V_{\text{c}}\in M_{Vc}$, $A_{\text{c}}\in M_{Ac}$, $J_{\text{U}}\in M_{J_{\text{U}}}$, $J_{\text{V}}\in M_{J_{\text{V}}}$, $R\in M_R$, $C_{\text{EV}}\in M_{C_{\text{EV}}}$, also for $y>0$, there is a corresponding value $z>0$ where $\|\eta S_{\text{c}}\|\leq z$, $\|\eta S_{\text{c}}\|\leq z$, $\|\eta V_{\text{c}}\|\leq z$, $\|\eta A_{\text{c}}\|\leq z$, $\|\eta J_{\text{U}}\|\leq z$, $\|\eta J_{\text{V}}\|\leq z$, $\|\eta R\|\leq z$, $\|\eta C_{\text{EV}}\|\leq z$. The subset of Banach space of all continuous functions on the interval $0\leq t\leq S$ are given as follows

$$
B_S=\left\{S_{\text{c}}\in\mathbb{H}^1([0,b],\mathbb{R}):\|S_{\text{c}}\|\leq y\right\},\ M_{Vc}=\left\{V\in\mathbb{H}^1([0,b],\mathbb{R}):\|V_{\text{c}}\|\leq y\right\},
$$

$$
M_{Ac}=\left\{A_{\text{c}}\in\mathbb{H}^1([0,b],\mathbb{R}):\|A_{\text{c}}\|\leq y\right\},\ M_{J_{\text{U}}}=\left\{J_{\text{U}}\in\mathbb{H}^1([0,b],\mathbb{R}):\|J_{\text{U}}\|\leq y\right\},
$$

$$
M_{J_{\text{V}}}=\left\{J_{\text{V}}\in\mathbb{H}^1([0,b],\mathbb{R}):\|J_{\text{V}}\|\leq y\right\},\ M_R=\left\{R\in\mathbb{H}^1([0,b],\mathbb{R}):\|R\|\leq y\right\},
$$

$$
B_{C_{\text{EV}}}=\left\{C_{\text{EV}}\in\mathbb{H}^1([0,b],\mathbb{R}):\|C_{\text{EV}}\|\leq y\right\}.
$$

Thus for any $0\leq t\leq S$,

$$
\begin{aligned}
\|\eta S_{\text{c}}\| &\leq \|S_c(0)\|+\frac{1}{\Gamma(\psi)}\int_0^t(t-\zeta)^{\psi-1}\|F(\zeta,S_{\text{c}}(\zeta))\|\,d\zeta\\
&\leq \|S(0)\|+\frac{\|F(\zeta,S_{\text{c}}(\zeta))\|}{\Gamma(\psi)}\int_0^t(t-\zeta)^{\psi-1}d\zeta\\
&\leq \|S(0)\|+L_{F1}\left(d+\|S_{\text{D}}\|\right)\left(\frac{\Gamma(1-\psi)\sin(\pi\psi)S^{\psi}}{\psi\pi}\right)\\
&\leq \|S(0)\|+L_{F1}(d+y)\left(\frac{\Gamma(1-\psi)\sin(\pi\psi)S^{\psi}}{\psi\pi}\right)=z.
\end{aligned}
$$

Applying the same method of solution, we have the following set of solutions.

$$\begin{aligned}
\|\eta V_{\mathrm{c}}\| &\leq \|V(0)\| + L_{G1}\,(d+y)\left(\frac{\Gamma(1-\psi)\sin(\pi\psi)S^{\psi}}{\psi\pi}\right),\\
\|\eta A_{\mathrm{c}}\| &\leq \|A(0)\| + L_{H1}\,(d+y)\left(\frac{\Gamma(1-\psi)\sin(\pi\psi)S^{\psi}}{\psi\pi}\right),\\
\|\eta J_{\mathrm{u}}\| &\leq \|J_{\mathrm{u}}(0)\| + L_{K1}\,(d+y)\left(\frac{\Gamma(1-\psi)\sin(\pi\psi)S^{\psi}}{\psi\pi}\right),\\
\|\eta J_{\mathrm{v}}\| &\leq \|J_{\mathrm{v}}(0)\| + L_{Q1}\,(d+y)\left(\frac{\Gamma(1-\psi)\sin(\pi\psi)S^{\psi}}{\psi\pi}\right),\\
\|\eta R\| &\leq \|R(0)\| + L_{U1}\,(d+y)\left(\frac{\Gamma(1-\psi)\sin(\pi\psi)S^{\psi}}{\psi\pi}\right),\\
\|\eta C_{\mathrm{EV}}\| &\leq \|C_{\mathrm{EV}}(0)\| + L_{W1}\,(d+y)\left(\frac{\Gamma(1-\psi)\sin(\pi\psi)S^{\psi}}{\psi\pi}\right).
\end{aligned}$$

Let Φ maps bounded set together with equal continuous sets in $\mathbb{H}^1\left([0,b],\mathbb{R}\right)$. Assuming that $0 \leq t_1 \leq t_2 \leq S$, $S_{\mathrm{c}} \in M_{Sc}$, $V_{\mathrm{c}} \in M_{Vc}$, $A_{\mathrm{c}} \in M_{Ac}$, $J_{\mathrm{u}} \in M_{J_{\mathrm{u}}}$, $J_{\mathrm{v}} \in M_{J_{\mathrm{v}}}$, $R{\in}M_R$, $C_{\mathrm{EV}} \in M_{C_{\mathrm{EV}}}$, with $t_1, t_2 \in [0,b]$, it follows that

$$\begin{aligned}
\|\eta S_{\mathrm{c}}(t_1) - \eta S_{\mathrm{c}}(t_2)\| &= \frac{1}{\Gamma(\psi)}\left\|\int_0^{t_1}(t_1-\zeta)^{\psi-1}F(\zeta,S_{\mathrm{c}}(\zeta)) - \int_0^{t_2}(t_2-\zeta)^{\psi-1}F(\zeta,S_{\mathrm{c}}(\zeta))\right\| d\zeta\\
&\leq \frac{1}{\Gamma(\psi)}\left\|\int_0^{t_1}\left((t_1-\zeta)^{\psi-1}-(t_2-\zeta)^{\psi-1}\right)F(\zeta,S_{\mathrm{c}}(\zeta))d\zeta\right\|\\
&\quad+\frac{1}{\Gamma(\psi)}\left\|\int_{t_1}^{t_2}(t_2-\zeta)^{\psi-1}F(\zeta,S_{\mathrm{c}}(\zeta))d\zeta\right\|\\
&\leq \frac{L_{F1}\,(d+y)}{\Gamma(\psi)}\left\|\int_0^{t_1}\left((t_1-\zeta)^{\psi-1}-(t_2-\zeta)^{\psi-1}\right)d\zeta+\int_{t_1}^{t_2}(t_2-\zeta)^{\psi-1}d\zeta\right\|\\
&\leq \left(\frac{L_{F1}\,(d+y)\,\Gamma(1-\psi)\sin(\pi\psi)}{\psi\pi}\right)\left(t_1^{\psi}-t_2^{\psi}+2(t_2-t_1)^{\psi}\right).
\end{aligned}$$

Applying the same method of solution, we have the following

$$\begin{aligned}
\|\eta V_{\mathrm{c}}(t_1) - \eta V_{\mathrm{c}}(t_2)\| &\leq \left(\frac{L_{G1}\,(d+y)\,\Gamma(1-\psi)\sin(\pi\psi)}{\psi\pi}\right)\left(t_1^{\psi}-t_2^{\psi}+2(t_2-t_1)^{\psi}\right),\\
\|\eta A_{\mathrm{c}}(t_1) - \eta A_{\mathrm{c}}(t_2)\| &\leq \left(\frac{L_{H1}\,(d+y)\,\Gamma(1-\psi)\sin(\pi\psi)}{\psi\pi}\right)\left(t_1^{\psi}-t_2^{\psi}+2(t_2-t_1)^{\psi}\right),\\
\|\eta J_{\mathrm{u}}(t_1) - \eta J_{\mathrm{u}}(t_2)\| &\leq \left(\frac{L_{K1}\,(d+y)\,\Gamma(1-\psi)\sin(\pi\psi)}{\psi\pi}\right)\left(t_1^{\psi}-t_2^{\psi}+2(t_2-t_1)^{\psi}\right),\\
\|\eta J_{\mathrm{v}}(t_1) - \eta J_{\mathrm{v}}(t_2)\| &\leq \left(\frac{L_{Q1}\,(d+y)\,\Gamma(1-\psi)\sin(\pi\psi)}{\psi\pi}\right)\left(t_1^{\psi}-t_2^{\psi}+2(t_2-t_1)^{\psi}\right),\\
\left\|\eta R_(t_1) - \eta R_(t_2)\right\| &\leq \left(\frac{L_{U1}\,(d+y)\,\Gamma(1-\psi)\sin(\pi\psi)}{\psi\pi}\right)\left(t_1^{\psi}-t_2^{\psi}+2(t_2-t_1)^{\psi}\right),\\
\|\eta C_{\mathrm{EV}}(t_1) - \eta C_{\mathrm{EV}}(t_2)\| &\leq \left(\frac{L_{W1}\,(d+y)\,\Gamma(1-\psi)\sin(\pi\psi)}{\psi\pi}\right)\left(t_1^{\psi}-t_2^{\psi}+2(t_2-t_1)^{\psi}\right).
\end{aligned}$$

As t_1 approaches t_2, the right-hand side of the inequalities approaches zero. The operator η is proven to be a continuous function using the Arzola-Ascoli theorem. Hitherto, the fact that η maps bounded sets together with another set has been shown. In addition to that, the operator is also continuous. Lastly, we would prove that $R(\eta) = \{(S_c, V_c, A_c, J_U, J_V R, C_{EV}) \in \mathbb{H}^1([0,b], \mathbb{R}) : (S_c, V_c, A_c, J_U, J_V, R, C_{EV}) = \Lambda(S_c, V_c, A_c, J_U, J_V, R, C_{EV})\}$ is bounded for some $\Lambda \in (0,1)$ using Lemma (1). Assuming that $(S_c, V_c, A_c, J_U, J_V, R, C_{EV},) \in R(\eta)$, so that
$(S_c, V_c, A_c, J_U, J_V, R, C_{EV}) = \Lambda\eta(S_c, V_c, A_c, J_U, J_V, R, C_{EV})$, it follows that for every $t \in [0,b]$ gives

$$\begin{aligned}
\|S_c(t)\| &\leq S_c(0) + \frac{1}{\Gamma(\psi)}\int_0^t (t-\zeta)^{\psi-1}\|F(\zeta, S_c(\zeta))\|\,d\zeta \\
&\leq S_c(0) + \frac{L_{F1}}{\Gamma(\psi)}\int_0^t (t-\zeta)^{\psi-1}(d + \|S_c(\zeta)\|)\,d\zeta \\
&\leq S_c(0) + \frac{cL_{F1}}{\Gamma(\psi)}\int_0^t (t-\zeta)^{\psi-1}\,d\zeta + \frac{L_{F1}}{\Gamma(\psi)}\int_0^t (t-\zeta)^{\psi-1}\|S_c(\zeta)\|\,d\zeta \\
&\leq S_c(0) + \left(L_{F1}\frac{\Gamma(1-\psi)\sin(\pi\psi)S^{\psi}}{\psi\pi}\right) + \left(\frac{L_{F1}\Gamma(1-\psi)\sin(\pi\psi)}{\pi}\right)\int_0^t (t-\zeta)^{\psi-1}\|S_c(\zeta)\|\,d\zeta \\
&\leq \left(S_c(0) + \frac{L_{F1}\Gamma(1-\psi)\sin(\pi\psi)S^{\psi}}{\psi\pi}E_{\psi}\left(L_{F1}T^{\psi}\right)\right) < \infty.
\end{aligned} \tag{24}$$

As already proven, $R(\eta)$ is bounded and using Schauder's fixed point theorem, the operator η has a fixed point and hence the solution of the fractional model.

Basic reproduction number of the model

To get the disease-free equilibrium (DFE) of the model, the right-hand side of the equations of the model (4) is set to zero which is as follows,

$$\xi_0 = (S_c(0), V_c(0), A_c(0), J_U(0), J_V(0), R(0), C_{EV}(0)) = \left(\frac{\Omega}{\delta+\mu}, \frac{\delta\Omega}{\mu(\delta+\mu)}, 0, 0, 0, 0, 0\right). \tag{25}$$

To get the linear stability of the disease-free equilibrium ξ_0, we apply the method of the next generation operator on the model (4). The matrix F (of new infection) and the matrix V (of the transfer of infections in and out of the disease compartments), respectively, are as follows

$$F = \begin{pmatrix} \frac{p\beta\omega Q_H}{N_H} & \frac{p\beta Q_H}{N_H} & \frac{p\beta\varrho_V Q_H}{N_H} & p\vartheta Q_H \\ \frac{(1-p)\beta\omega S_c}{N_H} & \frac{(1-p)\beta S_c}{N_H} & \frac{(1-p)\beta\varrho_V S_c}{N_H} & (1-p)\vartheta S_c \\ \frac{(1-f)(1-\xi)\beta\omega V_c}{N_H} & \frac{(1-f)(1-\xi)\beta V_c}{N_H} & \frac{(1-f)(1-\xi)\beta\varrho_V V_c}{N_H} & (1-f)(1-\xi)\vartheta V_c \\ 0 & 0 & 0 & 0 \end{pmatrix},$$

with $Q_H = S_c + f(1-\xi)V_c$,

$$V = \begin{pmatrix} \gamma_A + \mu & 0 & 0 & 0 \\ 0 & \gamma_{IU} + d_{JU} + \mu & 0 & 0 \\ 0 & 0 & \gamma_{IV} + d_{JV} + \mu & 0 \\ -\chi_1 & -\chi_2 & -\chi_3 & \mu_{EV} \end{pmatrix}.$$

Therefore, the basic reproduction number of the fractional order vaccination model for COVID-19 incorporating environmental transmission denoted by $\mathcal{R}_0 = \max\{\mathcal{R}_{0H}, \mathcal{R}_{0EV}\}$, where $\mathcal{R}_{0H}$ is human to human transmission, and $\mathcal{R}_{0\text{EV}}$ is environment to human transmission, respectively. The associated reproduction numbers are given by

$$\mathcal{R}_{0\text{H}} = \frac{\beta\omega\left(\theta_1\eta_A Q_H + (1-p)S_{\text{c}}^* + V_{\text{c}}^*\eta_v\right)}{N_H^* G_1 G_2 G_3},$$

and

$$\mathcal{R}_{0\text{EV}} = \frac{\beta\left(\chi_1 + (1-p)S_{\text{c}}^*\chi_2 + V_{\text{c}}^*\chi_3\right)}{\mu_{\text{EV}}},$$

where,

$$G_1 = \gamma_{\text{A}} + \mu, G_2 = \gamma_{\text{JU}} + d_{\text{JU}} + \mu, G_3 = \gamma_{\text{JV}} + d_{\text{JV}} + \mu, Q_H = S_{\text{c}}^* + f\left(1-\xi\right)V_{\text{c}}^*, V_{\text{c}} = (1-f)\left(1-\xi\right)V_{\text{c}}^*.$$

Local asymptomatic stability of the disease-free equilibrium

Theorem 4 *The condition for the DFE, N_0 of the model (4) to be locally asymptotically stable (LAS) is that the reproduction number must be less than 1, i.e $R_c < 1$, and unstable when the reproduction number is greater than 1, i.e $R_c > 1$.*

Proof To get the local stability of the model (4), we carried out the Jacobian matrix of the system (4) and computed it using the value gotten at the disease-free equilibrium given as follows:

$$\begin{pmatrix}
-(\mu+\delta) & 0 & \frac{-\beta\omega S_{\text{c}}^*}{N_H^*} & \frac{-\beta S_{\text{c}}^*}{N_H^*} & \frac{-\beta\varrho_v S_{\text{c}}^*}{N_H^*} & 0 & \vartheta S_{\text{c}}^* \\
\delta & -\mu & \frac{-(1-\xi)\beta\omega V_{\text{c}}^*}{N_H^*} & \frac{-(1-\xi)\beta V_{\text{c}}^*}{N_H^*} & \frac{-(1-\xi)\beta\varrho_v V_{\text{c}}^*}{N_H^*} & 0 & (1-\xi)\vartheta V_{\text{c}}^* \\
0 & 0 & \frac{p\beta\omega S_{\text{c}}^*+f)(1-\xi)\beta\omega V_{\text{c}}^*}{N_H^*} - G_1 & \frac{p\beta S_{\text{c}}^*+f(1-\xi)\beta V_{\text{c}}^*}{N_H^*} & \frac{p\beta\varrho_v S_{\text{c}}^*+f(1-\xi)\beta\varrho_{\text{V}} V_{\text{c}}^*}{N_H^*} & 0 & p\vartheta S_{\text{c}}^* + f(1-\xi)\vartheta V_{\text{c}}^* \\
0 & 0 & \frac{(1-p)\beta\omega S_{\text{c}}^*}{N_H^*} & \frac{(1-p)\beta S_{\text{c}}^*}{N_H^*} - G_2 & \frac{(1-p)\beta\varrho_v S_{\text{c}}^*}{N_H^*} & 0 & (1-p)\vartheta S_{\text{c}}^* \\
0 & 0 & \frac{(1-f)(1-\xi)\beta\omega V_{\text{c}}^*}{N_H^*} & \frac{(1-f)(1-\xi)\beta V_{\text{c}}^*}{N_H^*} & \frac{(1-f)(1-\xi)\beta\varrho_v V_{\text{c}}^*}{N_H^*} - G_3 & 0 & (1-f)(1-\xi)\vartheta V_{\text{c}}^* \\
0 & 0 & \gamma_{\text{A}} & \gamma_{\text{JU}} & \gamma_{\text{JV}} & -\mu & 0 \\
0 & 0 & \chi_1 & \chi_2 & \chi_3 & 0 & -\mu_{\text{EV}}
\end{pmatrix}.$$

The first four eigenvalues are $\lambda_1 = -(\mu+\delta), \quad \lambda_2 = -\mu(\text{twice}), \lambda_3 = -\mu_{\text{EV}}$, while the remaining three eigenvalues are obtained from the solutions of the equations below

$$(N_H + (-1+p)S_H\beta_1) - ((\lambda + G_2)V_H\beta_1\eta_v(1 - R_{0\text{P}})) - ((\lambda + G_2)(\lambda + G_3)Q_H\beta_1\eta_A\theta_1(1 - R_{0\text{C}})) = 0. \quad (26)$$

Following the method of the Routh-Hurwitz, the above equations will possess roots with negative real parts $\iff \mathcal{R}_{0\text{H}} < 1$ and $\mathcal{R}_{0\text{EV}} < 1$ respectively. Hence, the DFE $J(N_0)$ is locally asymptotically stable if $R_0 = \max\{\mathcal{R}_{0\text{H}}, \mathcal{R}_{0\text{EV}}\} < 1$.

Epidemiologically, the above result implies that the prevalence of COVID-19 can be eradicated from the population provided $R_0 < 1$ and if the initial sizes of the population of the model are in the region of attraction of the DFE.

Generalized Ulam-Hyers-Rassias stability

In this section, the approach by Liu [30] shall be applied to prove that the fractional model is generalized UHR stable. Following [30], the definition below holds:

Definition 6 *The fractional model (4)- (5) is generalized Ulam-Hyers-Rassias (UHR) stable with regards to $\Upsilon(t) \in \mathbb{H}^1([0,b],\mathbb{R})$ provided there is a real value $\Sigma_\psi > 0$ so that $\epsilon > 0$ and for every solution*

$(S_c, V_c, A_c, J_u, J_v, R, C_{ev},) \in \mathbb{H}^1([0,b], \mathbb{R})$ *of the inequalities below*

$$\left|D_t^{\psi} S_c(t) - F(t, S_c(t))\right| \leq \Upsilon(t), \quad \left|D_t^{\psi} V_c(t) - G(t, V_c(t))\right| \leq \Upsilon(t), \quad \left|D_t^{\psi} A_c(t) - H(t, A_c(t))\right| \leq \Upsilon(t),$$

$$\left|D_t^{\psi} J_u(t) - K(t, J_u(t))\right| \leq \Upsilon(t), \quad \left|D_t^{\psi} J_v(t) - Q(t, J_v(t))\right| \leq \Upsilon(t), \quad \left|D_t^{\psi} R(t) - U(t, R(t))\right| \leq \Upsilon(t),$$

$$\left|D_t^{\psi} C_{ev}(t) - W(t, C_{ev}(t))\right| \leq \Upsilon(t),$$

there is a solution $(\bar{S}_c, \bar{V}_c, \bar{A}_c, \bar{J}_u, \bar{J}_v, \bar{R}, \bar{C}_{ev}) \in \mathbb{H}^1([0,b], \mathbb{R})$ *of the fractional model* (4)-(5) *with*

$$\left|S_c(t) - \bar{S}_c(t)\right| \leq \Sigma_{\psi}\Upsilon(t), \left|V_c(t) - \bar{V}_c(t)\right| \leq \Sigma_{\psi}\Upsilon(t), \left|A_c(t) - \bar{A}_c(t)\right| \leq \Sigma_{\psi}\Upsilon(t), \left|J_u(t) - \bar{J}_u(t)\right| \leq \Sigma_{\psi}\Upsilon(t),$$

$$\left|J_v(t) - \bar{J}_v(t)\right| \leq \Sigma_{\psi}\Upsilon(t), \left|R(t) - \bar{R}(t)\right| \leq \Sigma_{\psi}\Upsilon(t), \quad \left|C_{ev}(t) - \bar{C}_{ev}(t)\right| \leq \Sigma_{\psi}\Upsilon(t).$$

Theorem 5 *The fractional model* (4)- (5) *is generalized Ulam-Hyers-Rassias stable with regards to* $\Upsilon \in \mathbb{H}^1([0,b], \mathbb{R})$ *if* $\left(L_F, L_G, L_H, L_K, L_Q, L_U, L_W\right) S^{\psi} < 1$.

Proof From definition (6), let Υ stand for the non-decreasing function of t, then there is $\epsilon > 0$ so that

$$\int_0^t (t-\zeta)^{\psi-1}\Upsilon(\zeta)d\zeta \leq \epsilon\Upsilon(t),$$

for every $t \in [0,b]$. The functions F, G, H, K, Q, U, W according to prove is said to be continuous and

$$(L_F, L_G, L_H, L_K, L_Q, L_U, L_W) > 0$$

meets the Lipschitz condition as seen in the previous part. From Theorem (2), the fractional model (4)- (5) has the unique solution

$$\bar{S}_c(t) = S_c(0) + \frac{1}{\Gamma(\psi)}\int_0^t (t-\zeta)^{\psi-1}F(\zeta, \bar{S}_c(\zeta))d\zeta.$$

Integrating the inequalities in definition (6) we get

$$\begin{aligned} \left|S_c(t) - S_c(0) - \frac{1}{\Gamma(\psi)}\int_0^t (t-\zeta)^{\psi-1}F(\zeta, S_c(\zeta))d\zeta\right| &\leq \frac{1}{\Gamma(\psi)}\int_0^t (t-\zeta)^{\psi-1}\Upsilon(\zeta)d\zeta \\ &\leq \frac{\epsilon\Upsilon(t)\Gamma(1-\psi)\sin(\pi\psi)}{\pi}. \end{aligned} \tag{27}$$

Using Lemma (1) and Eq. (27), we have the following

$$\begin{aligned}
\left|S_c(t)-\bar{S}_c(t)\right| &\le \left|S_c(t)-\left(S_c(0)+\frac{1}{\Gamma(\psi)}\int_0^t (t-\zeta)^{\psi-1}F(\zeta,\bar{S}_c(\zeta))d\zeta\right)\right| \\
&\le \left|S_c(t)-S_c(0)-\left(\frac{1}{\Gamma(\psi)}\int_0^t (t-\zeta)^{\psi-1}F(\zeta,\bar{S}_c(\zeta))d\zeta+\frac{1}{\Gamma(\psi)}\int_0^t (t-\zeta)^{\psi-1}F(\zeta,S_c(\zeta))d\zeta\right.\right. \\
&\quad \left.\left.-\frac{1}{\Gamma(\psi)}\int_0^t (t-\zeta)^{\psi-1}F(\zeta,S_c(\zeta))d\zeta\right)\right| \\
&\le \left|S_c(t)-S_c(0)-\frac{1}{\Gamma(\psi)}\int_0^t (t-\zeta)^{\psi-1}F(\zeta,S_c(\zeta))d\zeta\right| \\
&\quad +\frac{1}{\Gamma(\psi)}\int_0^t (t-\zeta)^{\psi-1}\left|F(\zeta,S(\zeta))-F(\zeta,\bar{S}_c(\zeta))\right|d\zeta \\
&\le \frac{\epsilon\Upsilon(t)\Gamma(1-\psi)\sin(\pi\psi)}{\pi}+\frac{L_F\Gamma(1-\psi)\sin(\pi\psi)}{\pi}\int_0^t (t-\zeta)^{\psi-1}\left|S_c(\zeta)-\bar{S}_c(\zeta)\right|d\zeta \\
&\le \frac{\epsilon\Upsilon(t)\Gamma(1-\psi)\sin(\pi\psi)}{\pi}E_\psi\left(L_F S^\psi\right).
\end{aligned}$$

By setting $\Sigma_\psi = \frac{\epsilon\Gamma(1-\psi)\sin(\pi\psi)}{\pi}E_\psi\left(L_F S^\psi\right)$ we have

$$\left|S_c(t)-\bar{S}_c(t)\right| \le \Sigma_\psi\Upsilon(t), \qquad t\in[0,b].$$

Using the method of solution, we have the following

$$\left|V_c(t)-\bar{V}_c(t)\right| \le \Sigma_\psi\Upsilon(t),\ \left|A_c(t)-\bar{A}_c(t)\right| \le \Sigma_\psi\Upsilon(t),\ \left|J_u(t)-\bar{J}_u(t)\right| \le \Sigma_\psi\Upsilon(t),$$

$$\left|J_v(t)-\bar{J}_v(t)\right| \le \Sigma_\psi\Upsilon(t),\ \left|R(t)-\bar{R}(t)\right| \le \Sigma_\psi\Upsilon(t),\ \left|C_{EV}(t)-\bar{C}_{EV}(t)\right| \le \Sigma_\psi\Upsilon(t),$$

for every $t\in[0,b]$. Therefore, it is concluded that the fractional model is generalized Ulam-Hyers-Rassias stable with regards to $\Upsilon(t)$. ■

4 Numerical scheme and simulations

On account of the many benefits of the fractional predictor-corrector technique, it is applied in this section to numerically solve the proposed model. The numerical scheme is derived from the Adams-Bashforth linear multi-step method in the Caputo sense [34] The numerical method's convergence was also a topic of discussion. The entire model (4)-(5) is simulated using the values of the parameters listed in our table 2 in accordance with the demographic and epidemiological data pertinent to the dynamics of COVID-19 incorporating environmental transmission in Nigeria. The total population of Nigeria is roughly 206,139,587, and the average lifespan in Nigeria is 54.69 years [31]. we have that $\mu = \frac{1}{54.69} \approx 0.0183 \quad year^{-1}$ and $\Omega = \mu \times 200,000,000 \approx 365,6976 \quad year^{-1}$. The initial conditions are put as listed as: $S_c(0) = 200,000,000, V_c(0) = 5000000, A_c(0) = 5000, J_u(0) = 2000, J_v(0) = 2000, R(0) = 2000, C_{EV}(0) = 2500$.

Let $t_k = kh, k = 0,1,2,\ldots,m$ be the uniform grid points with some integer m and $h = T/m$, which is the grid step size. As a result, (4) reduces to the fractional version of the one-step Adam-Moulton method (Corrector formula) which is obtained by employing piece-wise interpolation with nodes and knots located at $t_j, j = 0,1,2,\ldots,k+1$,

$$
\begin{aligned}
S_{\text{c}}(t_{r+1}) - S_{\text{c}}(0) &= \frac{g^{\psi}}{\Gamma(\psi+2)}\left(\sum_{i=0}^{r} u_{i,r+1} F\left(t_i, S_{\text{c}}(t_i)\right) + F\left(t_{r+1}, S^{q}_{\text{c}}(t_{r+1})\right)\right), \\
V_{\text{c}}(t_{r+1}) - V_{\text{c}}(0) &= \frac{g^{\psi}}{\Gamma(\psi+2)}\left(\sum_{i=0}^{r} u_{i,r+1} G\left(t_i, V_{\text{c}}(t_i)\right) + G\left(t_{r+1}, V^{q}_{\text{c}}(t_{r+1})\right)\right), \\
A_{\text{c}}(t_{r+1}) - A_{\text{c}}(0) &= \frac{g^{\psi}}{\Gamma(\psi+2)}\left(\sum_{i=0}^{r} u_{i,r+1} H\left(t_i, A_{\text{c}}(t_i)\right) + H\left(t_{r+1}, A^{q}_{\text{c}}(t_{r+1})\right)\right), \\
J_{\text{U}}(t_{r+1}) - J_{\text{U}}(0) &= \frac{g^{\psi}}{\Gamma(\psi+2)}\left(\sum_{i=0}^{r} u_{i,r+1} K\left(t_i, J_{\text{U}}(t_i)\right) + K\left(t_{r+1}, J^{q}_{\text{U}}(t_{r+1})\right)\right), \qquad (28) \\
J_{\text{V}}(t_{r+1}) - J_{\text{V}}(0) &= \frac{g^{\psi}}{\Gamma(\psi+2)}\left(\sum_{i=0}^{r} u_{i,r+1} Q\left(t_i, J_{\text{V}}(t_i)\right) + Q\left(t_{r+1}, J^{q}_{\text{U}}(t_{r+1})\right)\right), \\
R(t_{r+1}) - R(0) &= \frac{g^{\psi}}{\Gamma(\psi+2)}\left(\sum_{i=0}^{r} u_{i,r+1} U\left(t_i, R(t_i)\right) + U\left(t_{r+1}, R^{q}(t_{r+1})\right)\right), \\
C_{\text{EV}}(t_{r+1}) - C_{\text{EV}}(0) &= \frac{g^{\psi}}{\Gamma(\psi+2)}\left(\sum_{i=0}^{r} u_{i,r+1} V\left(t_i, C_{\text{EV}}(t_i)\right) + W\left(t_{r+1}, C^{q}_{\text{EV}}(t_{r+1})\right)\right),
\end{aligned}
$$

where the weight $u_{i,r+1} = \begin{cases} r^{\psi+1} - (r-\psi)(r+1)^{\psi}, & i = 0. \\ (r-i+2)^{\psi+1} + (r-i)^{\psi+1} - 2\left(r-i+1\right)^{\psi+1}, & 1 \le i \le r. \\ 1, & i = r+1. \end{cases}$

The predictor formula motivated by the well-known one-step Adam-Bashforth method is given by

$$
\begin{aligned}
S^{q}_{\text{c}}\left(t_{r+1}\right) - S_{\text{c}}(0) &= \frac{1}{\Gamma\left(\psi\right)} \sum_{i=0}^{r} v_{i,r+1} F\left(t_i, S_{\text{c}}(t_i)\right), \\
V^{q}_{\text{c}}(t_{r+1}) - V_{\text{c}}(0) &= \frac{1}{\Gamma\left(\psi\right)} \sum_{i=0}^{r} v_{i,r+1} G\left(t_i, V_{\text{c}}(t_i)\right), \\
A^{q}_{\text{c}}(t_{r+1}) - A_{\text{c}}(0) &= \frac{1}{\Gamma\left(\psi\right)} \sum_{i=0}^{r} v_{i,r+1} H\left(t_i, A_{\text{c}}(t_i)\right), \qquad (29) \\
J^{q}_{\text{U}}(t_{r+1}) - J_{\text{U}}(0) &= \frac{1}{\Gamma\left(\psi\right)} \sum_{i=0}^{r} v_{i,r+1} K\left(t_i, J_{\text{U}}(t_i)\right), \\
J^{q}_{\text{V}}(t_{r+1}) - J_{\text{V}}(0) &= \frac{1}{\Gamma\left(\psi\right)} \sum_{i=0}^{r} v_{i,r+1} Q\left(t_i, J_{\text{V}}(t_i)\right), \\
R^{q}\left(t_{r+1}\right) - R(0) &= \frac{1}{\Gamma\left(\psi\right)} \sum_{i=0}^{r} v_{i,r+1} U\left(t_i, R(t_i)\right), \\
C^{q}_{\text{EV}}\left(t_{r+1}\right) - C_{\text{EV}}(0) &= \frac{1}{\Gamma\left(\psi\right)} \sum_{i=0}^{r} v_{i,r+1} W\left(t_i, C_{\text{EV}}(t_i)\right),
\end{aligned}
$$

where the weight is given by

$$v_{i,r+1} = \psi^{-1} g^{\psi} \left((r-i+1)^{\psi} - (r-i)^{\psi} \right).$$

Model fitting

The genetic algorithm method was used to fit the model in accordance with [35], which specifies the values for the parameters under investigation. The above investigation was carried out using the *fmincon* function in the optimization toolbox of MATLAB. Figure 1 presents the fitting of the model 4. It was applied to the weekly total number of COVID-19 cases that had been confirmed in Nigeria between April 1, 2021, and June 10, 2021. The figure demonstrates that the model behaves very similarly to Nigeria's COVID-19 data. The table provides a rough estimate of additional fitting-derived parameters.1.

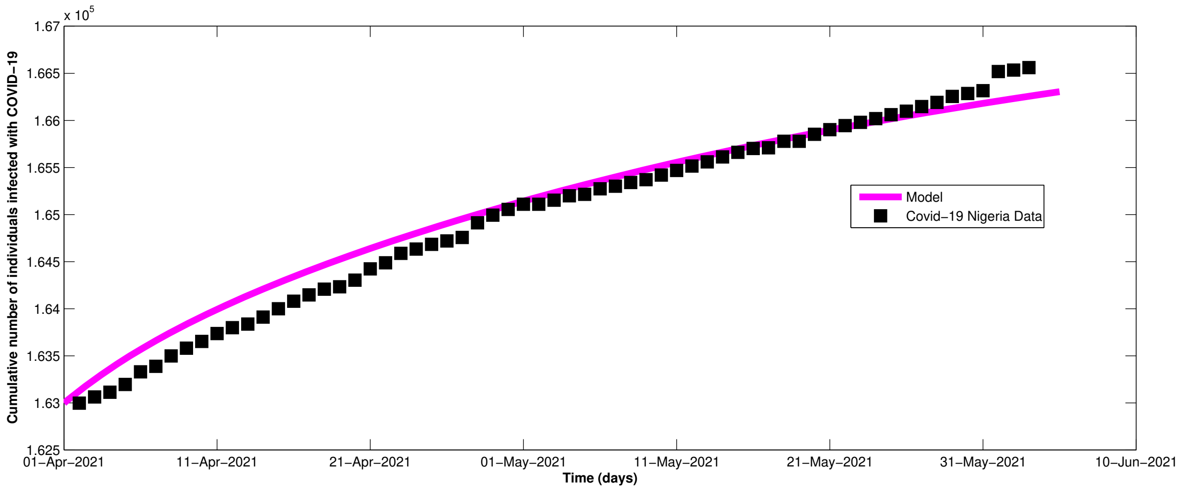

Figure 1. Fitting the model to the cumulative number of confirmed COVID-19 cases in Nigeria. All other parameters are as in Table 1

Impact of different values of fractional order on the model classes

Figure 1 presents simulations of the susceptible class at various fractional orders. During the first 35 days of the simulation, it is observed that the total population grows as the fractional order decreases and that the trend reverses as the fractional order increases. The simulations of the vaccinated class at various fractional orders are shown in Figure 2. A comparative pattern is noticed; The total population rises while the fractional order decreases during the first quarter of the simulation period (35 days). As the fractional grows, the total population then shifts in the opposite direction. The simulations for the Asymptomatic class are shown in Figure 3; For the first quarter of the simulation period, it is observed that the total population does not increase or decrease when the fractional order decreases. By the by, accordingly, it increments and diminishes eventually as the fractional order diminishes. The simulations for the unvaccinated asymptomatic class are shown in Figure 4; it shows that for the initial 30 days of the simulations time frame, a decline in the fractional order value leaves the population unaltered as there was neither an increment nor a diminishing in the complete population. As the fractional order decreased, there was an increase in the total population.

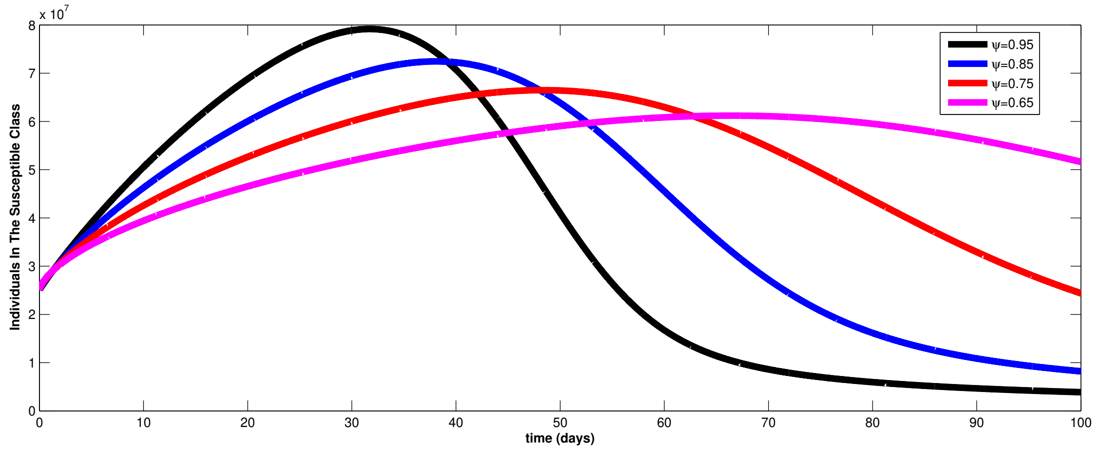

Figure 2. Simulations of the Susceptible individuals at different fractional order values. All other parameters as in Table 1

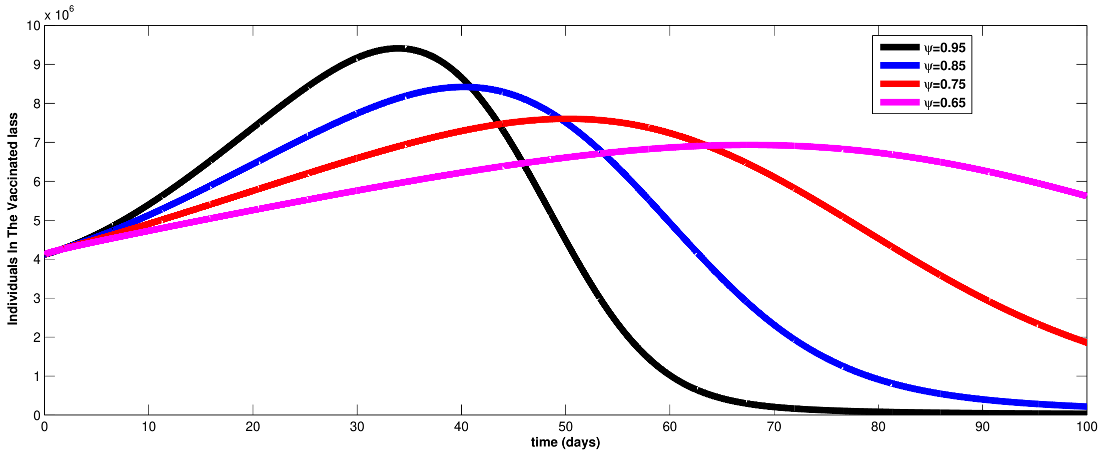

Figure 3. Simulations of the Vaccinated individuals at different fractional order values. Using additional parameters from Table 1

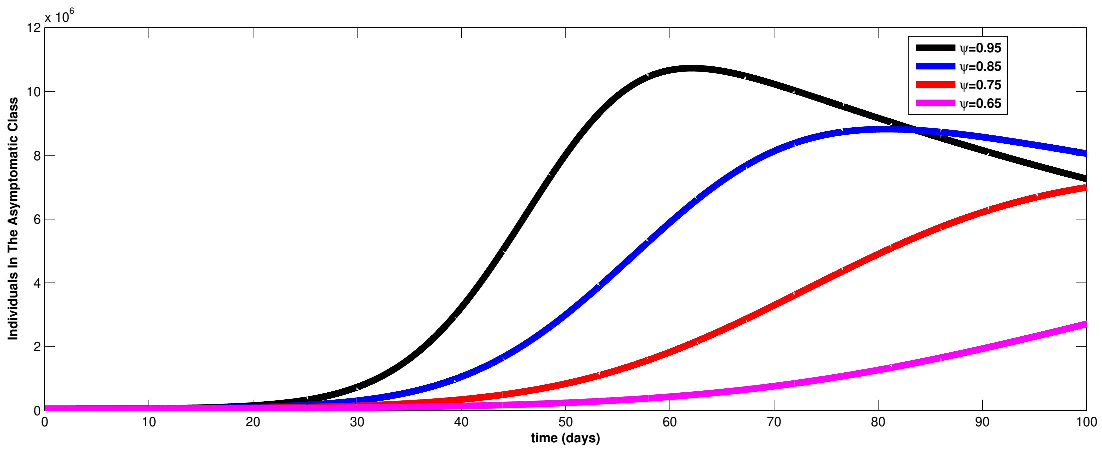

Figure 4. Simulations of the Asymptomatic individuals at different fractional order values. Using additional parameters from Table 1

Figure 5 presents the simulations of the vaccinated asymptomatic class; During the first forty days of the simulation, it is observed that the fractional order decreases while the total population increases slightly; After that, the fractional order decreases, resulting in a significant increase in the total population. The simulations for the Recovered class are shown in Figure 6; for the first 40 days of the simulations, it is observed that the total population does not change as the fractional order decreases; rather, it does not increase or decrease. Nonetheless, following a decline in the fractional order, there was an expansion in the complete population. The simulations of the environment's COVID-19 concentration are shown in Figure 7; the simulations demonstrate that as the fractional order decreased, neither an increase nor a decrease in the total population occurred; as a result, the total population increased as the fractional order decreased.

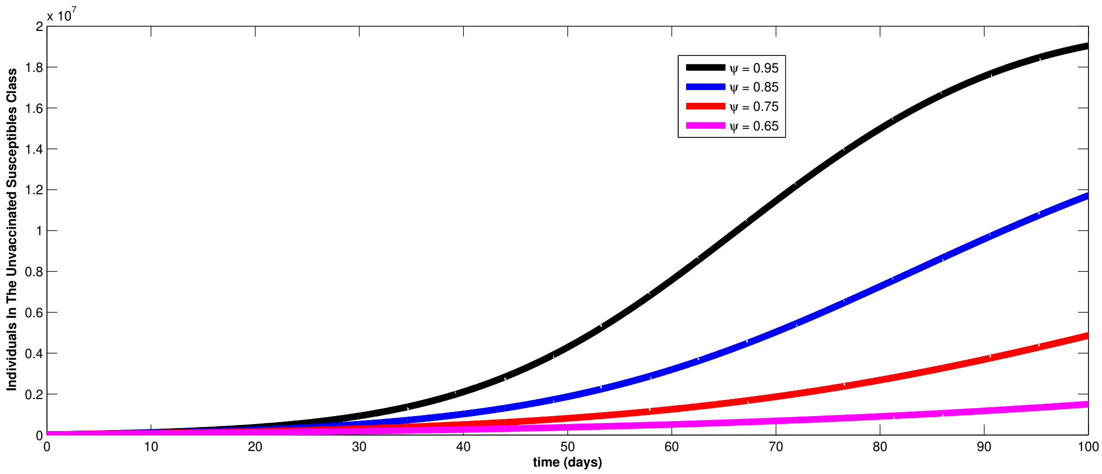

Figure 5. Simulations of the unvaccinated susceptible individuals at different fractional order values. Using additional parameters from Table 1

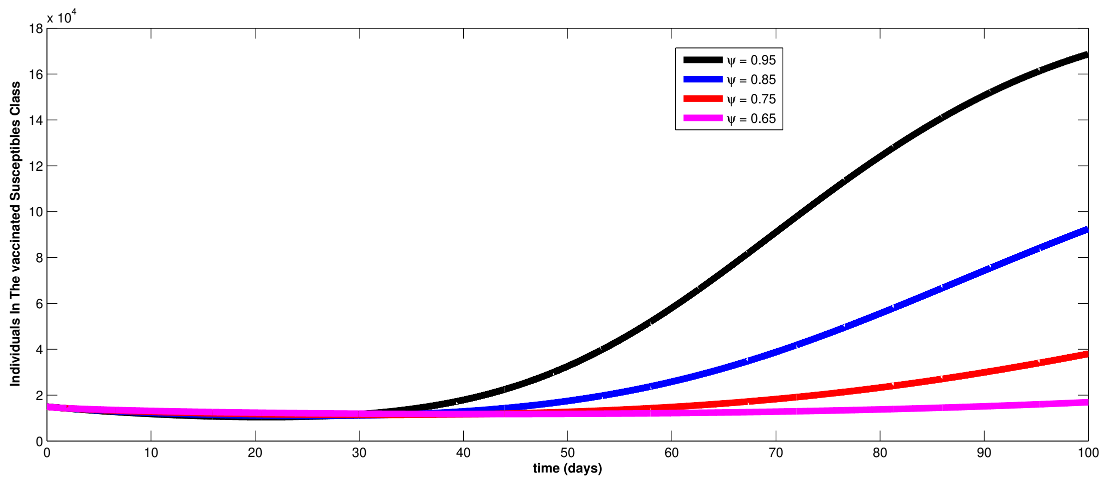

Figure 6. Simulations of the vaccinated susceptible individuals at different fractional order values. Using additional parameters from Table 1

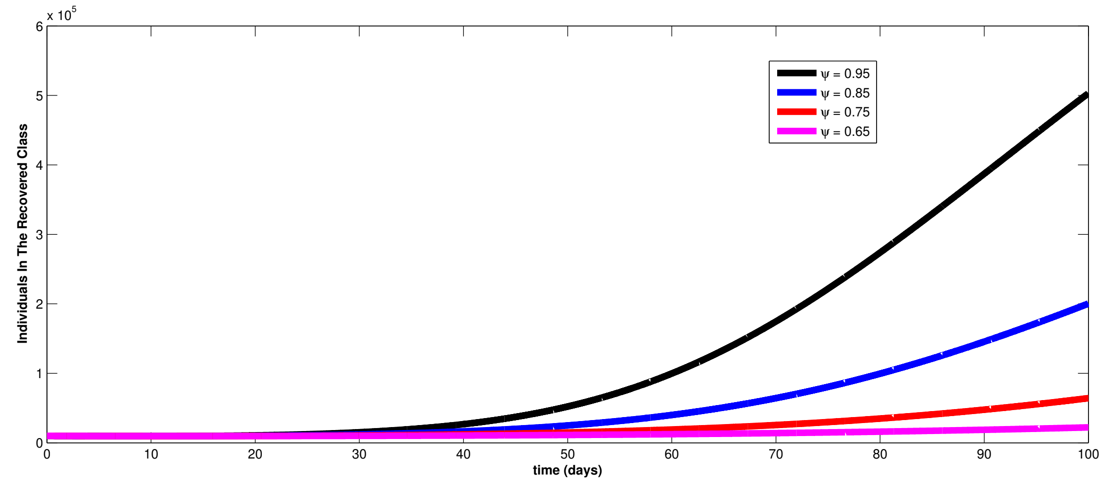

Figure 7. Simulations of the Recovered individuals at different fractional order values. Using additional parameters from Table 1

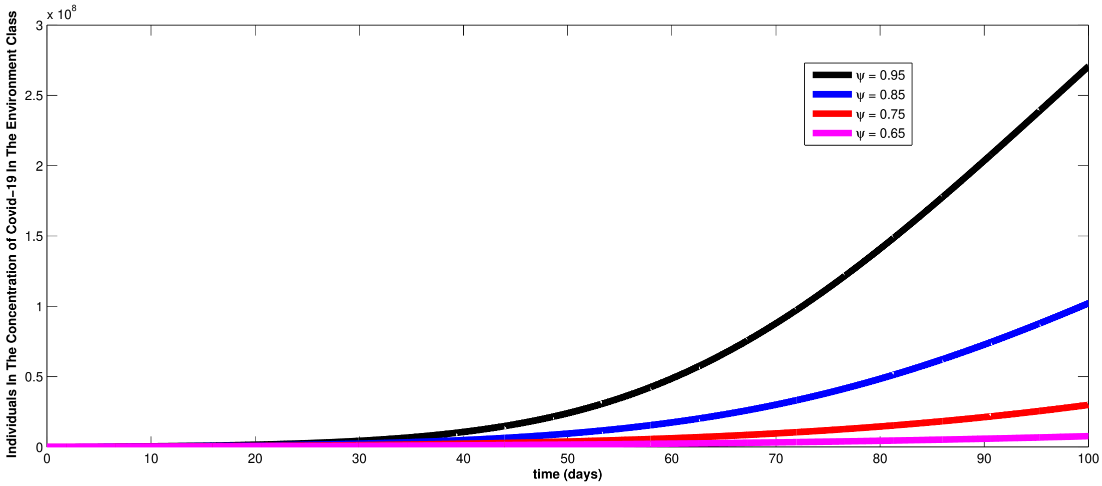

Figure 8. Simulations of the concentration of COVID-19 in the environment at different fractional order values. Using additional parameters from Table 1

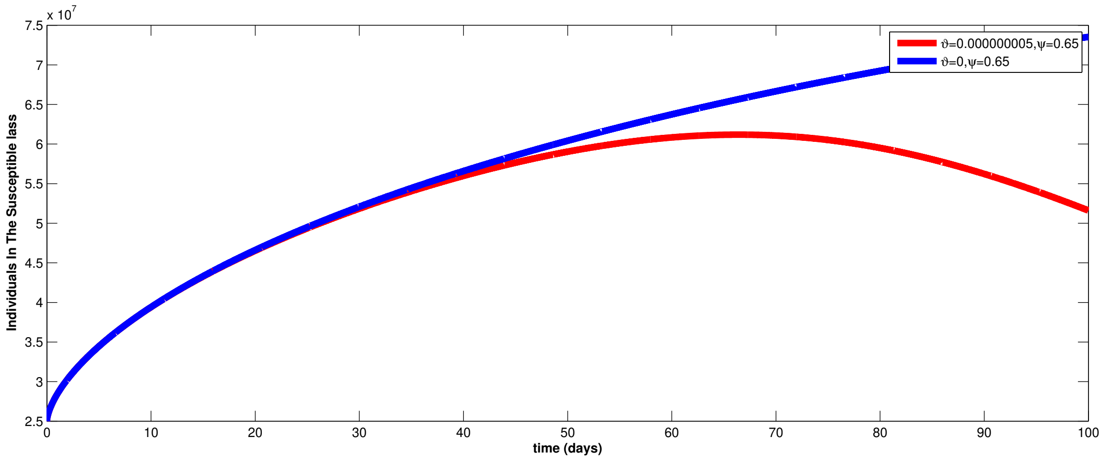

Figure 9. Simulation of the susceptible individual in the presence and absence of environmental transmission of COVID-19. Here, $\psi = 0.65$. Using additional parameters from Table 1

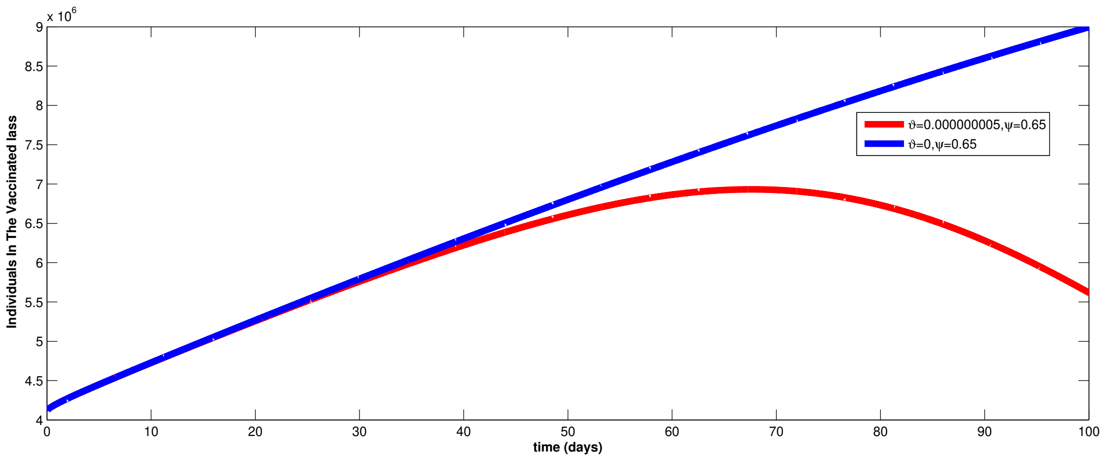

Figure 10. Simulation of the vaccinated individual in the presence and absence of environmental transmission of COVID-19. Here, $\psi = 0.65$. Using additional parameters from Table 1

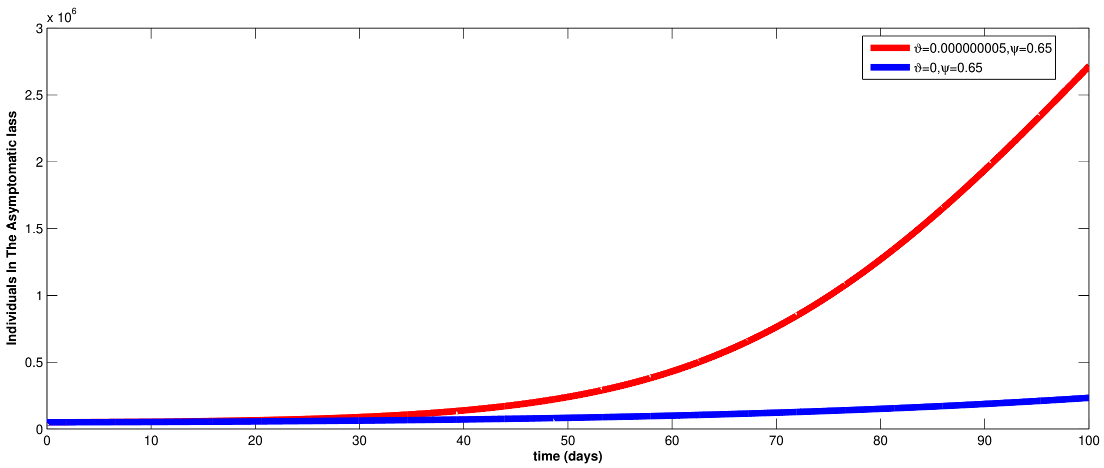

Figure 11. Simulation of the asymptomatic susceptible individual in the presence and absence of environmental transmission of COVID-19. Here, $\psi = 0.65$. Using additional parameters from table 1

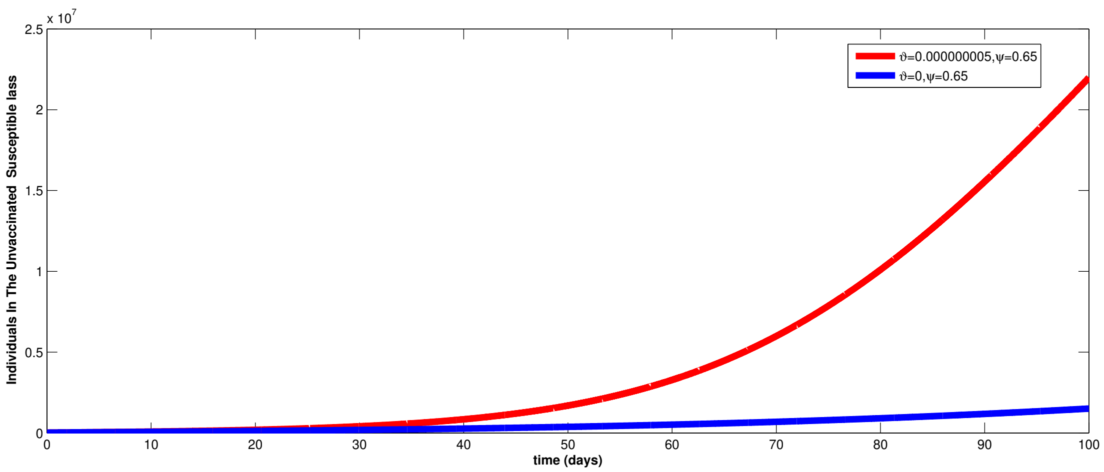

Figure 12. Simulation of the unvaccinated susceptible individual in the presence and absence of environmental transmission of COVID-19. Here, $\psi = 0.65$. Using additional parameters from Table 1

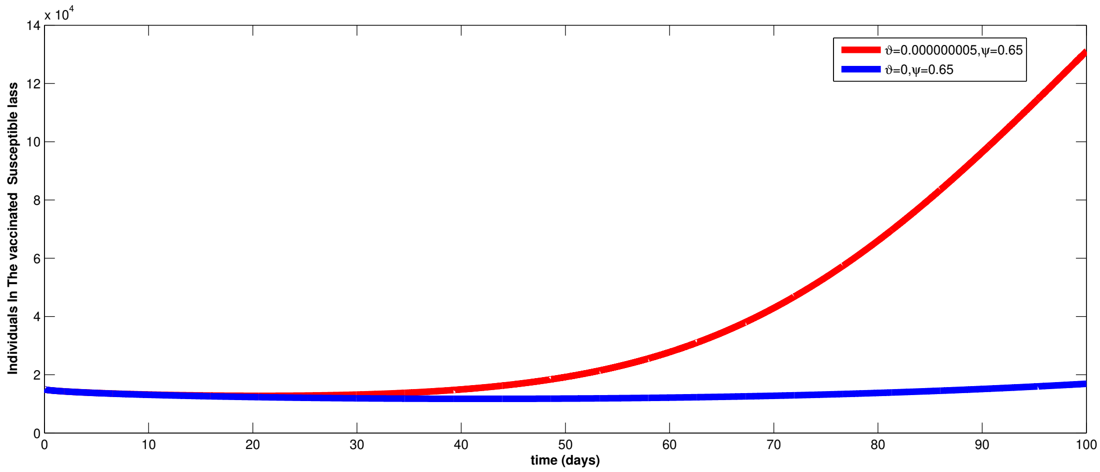

Figure 13. Simulation of the vaccinated susceptible individual in the presence and absence of environmental transmission of COVID-19. Here, $\psi = 0.65$. Using additional parameters from Table 1

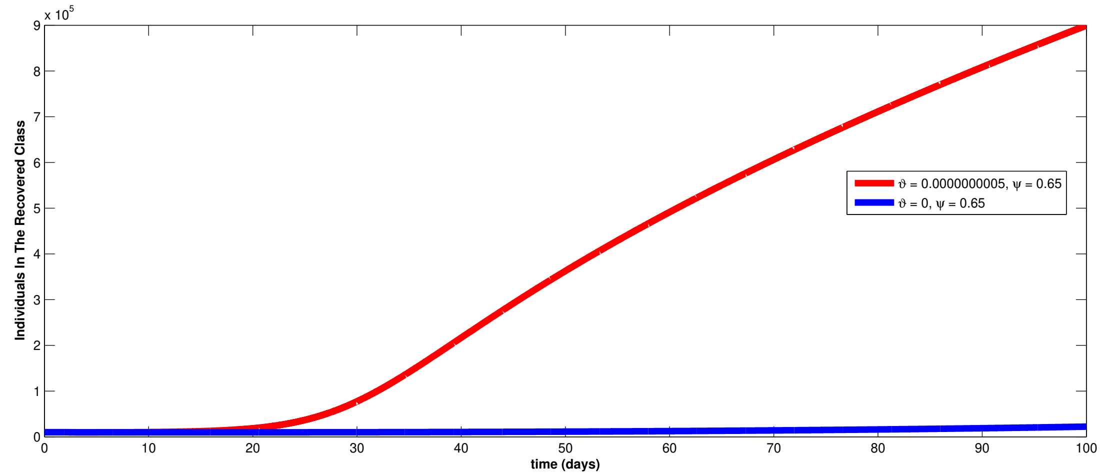

Figure 14. Simulation of vaccinated Recovered individual in the presence and absence of environmental transmission of COVID-19. Here, $\psi = 0.65$. Using additional parameters from Table 1

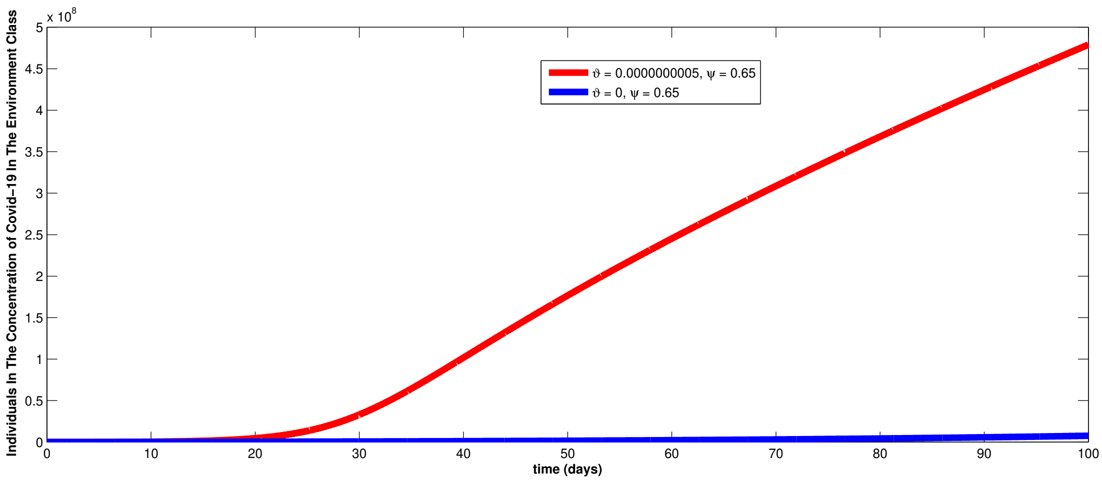

Figure 15. Simulation of concentration of COVID-19 in the environment in the presence and absence of environmental transmission of COVID-19. Here, $\psi = 0.65$. Using additional parameters from Table 1

Impact of environmental transmission on the model classes

Figure 8 presents the simulations of the susceptible individuals in the presence and absence of environmental transmission of Coronavirus. It has been carefully observed that when there is no environmental transmission, the population grows because there are no infected people and that is because the population is made up of people who are susceptible. However, the number of asymptomatic individuals exposed to COVID-19 rises as environmental transmission decreases the population.
In Figure 9, the simulations of the vaccinated individuals in the presence and absence of environmental transmission are introduced. When there is no environmental transmission, the population as a whole grows because there is no infection. On the other hand, when there is environmental transmission, the population as a whole shrinks dramatically, leading to an increase in the number of people who are asymptomatic after coming into effective contact with the infected environment. The simulations of the asymptomatic individuals in the presence and absence of environmental transmission are shown in Figure 10.
The shortfall of environmental transmission shows no impact on the absolute population for the initial 40 days of the simulations time frame yet somewhat increments after the primary period, this is on the grounds that the class is as of now an infected class that shows no side effects. The infection grows rather than decreases as a result of environmental transmission; For the first quarter of the simulation, the presence of environmental transmission has no effect on asymptomatic individuals; however, after the first simulation period, the number of symptomatic individuals rises.
In Figure 11, the simulations of the unvaccinated asymptomatic individuals in the presence and absence of environmental transmission are introduced; at the point when there is no environmental transmission, for the principal quarter of the simulations time frame, the people in the class neither increments nor diminishes however marginally expanded after the primary period, this is on the grounds that it is now an infected class, so the shortfall of environmental transmission does not influence the class, yet when there is an environmental transmission, the class stay unaltered for the main quarter of the reproductions time frame yet increments after the primary time of the simulations.
The simulations of the vaccinated asymptomatic individuals in the presence and absence of environmental transmission are shown in Figure 12; at the point when there is no environmental transmission, it somewhat builds the quantity of the asymptomatic individual, yet when there is an environmental transmission, we have a larger number of asymptomatic people. The simulations of the Recovered individuals with and without environmental transmission are shown in Figure 13.
The absence of environmental transmission is observed to have no effect on the class. However, after 20 days of simulation, there are more asymptomatic individuals in the presence of environmental transmission. In Figure 14, the simulations of the concentration of Coronavirus in the environment are introduced. It is observed that when there is no environmental transmission, the class stay unaltered for the initial 20 days of the simulations time frame. At the point when there is environmental transmission, the quantity of the asymptomatic people fundamentally expanded following 20 days.

5 Conclusion

The fractional derivative was used to consider and analyze a fractional-order vaccination model for COVID-19 incorporating environmental transmission. The Mittag-Leffler function is used to demonstrate the solutions' positivity and boundedness. The existence and uniqueness of the

model solutions are additionally shown utilizing Banach and Schauder's fixed point theorem. In addition, we demonstrate the Ulam-Hyers-Rassias stability of the fractional-order model. For the locally asymptotically stable system, it was demonstrated that the reproduction number was lower than unity. Numerical simulations were likewise viewed as utilizing information pertinent to Coronavirus cases for Nigeria and fitted to the week-by-week combined number of affirmed cases from April 1, 2021, to June 10, 2021, to look at the effect of various fractional order values on the model classes and the effect of environmental transmission on the model classes.
The highlights of the simulations are as follows:
(i) As depicted in Figure 2, the fractional-order value decreases with increasing model class population.
(ii) There is a larger overall population when there is no environmental transmission. The number of people who are asymptomatic rises when there is environmental transmission, as shown in Figure 9.

Declarations

Ethical approval

Not applicable.

Consent for publication

Not applicable.

Conflicts of interest

The authors declare that they have no conflict of interest.

Funding

Not applicable.

Author's contributions

A.O.A.: Conceptualization, Software, Formal Analysis, Validation, Visualization, Data Curation, Writing-Original draft. A.O.: Methodology, Supervision, Writing-Review and Editing. S.C.I.: Supervision, Review. All authors discussed the results and contributed to the final manuscript.

Acknowledgements

Not applicable.

References

[1] Kahn, J.S. and McIntosh, K. History and recent advances in coronavirus discovery. *The Pediatric Infectious Disease Journal*, 24(11), S223-S227, (2005). [CrossRef]

[2] Bhargava HD, WebMD Medical Reference, August 15, (2021).

[3] WMCH Wuhan Municipal Health and Health Commission's Briefing on the Current Pneumonia Situation in our City, February 1, (2020).

[4] World Health Organization (WHO), URL: https://www.who.int/health-topics/coronavirus, (2021). (Access Date: February 2023).

[5] Viner, R.M., Mytton, O.T., Bonell, C., Melendez-Torres, G.J., Ward, J., et al. Susceptibility to SARS-CoV-2 infection among children and adolescents compared with adults: a systematic review and meta-analysis. *JAMA Pediatrics*, 175(2), 143-156, (2021). [CrossRef]

[6] Koh, W.C., Naing, L., Chaw, L., Rosledzana, M.A., Alikhan, M.F., Jamaludin, S.A., et al. What do we know about SARS-CoV-2 transmission? A systematic review and meta-analysis of the secondary attack rate and associated risk factors. *PLoS one*, 15(10), e0240205, (2020). [CrossRef]

[7] https://www.ncdc.gov.ng/coronavirus, (2021). (Access Date: November 2022).

[8] Ahmed, I., Modu, G.U., Yusuf, A., Kumam, P. and Yusuf, I. A mathematical model of Coronavirus Disease (COVID-19) containing asymptomatic and symptomatic classes. *Results in Physics*, 21, 103776, (2021). [CrossRef]

[9] Omame, A., Abbas, M. and Onyenegecha, C.P. A fractional-order model for COVID-19 and tuberculosis co-infection using Atangana–Baleanu derivative. *Chaos, Solitons & Fractals*, 153, 111486, (2021). [CrossRef]

[10] Bugalia, S., Bajiya, V.P., Tripathi, J.P., Li, M.T. and Sun, G.Q. Mathematical modeling of COVID-19 transmission: the roles of intervention strategies and lockdown. *Mathematical Biosciences and Engineering*, 17(5), 5961-5986, (2020). [CrossRef]

[11] Iboi, E.A., Sharomi, O., Ngonghala, C.N., & Gumel, A.B. Mathematical modeling and analysis of COVID-19 pandemic in Nigeria. *Mathematical Biosciences and Engineering*, 17(6), 7192-7220, (2020). [CrossRef]

[12] Okuonghae, D. and Omame, A. Analysis of a mathematical model for COVID-19 population dynamics in Lagos, Nigeria. *Chaos, Solitons & Fractals*, 139, 110032, (2020). [CrossRef]

[13] Baba, B. A. and Bilgehan, B. Optimal control of a fractional order model for the COVID–19 pandemic. *Chaos, Solitons & Fractals*, 144, 110678, (2021). [CrossRef]

[14] Aba Oud, M.A., Ali, A., Alrabaiah, H., Ullah, S., Khan, M.A. and Islam, S. A fractional order mathematical model for COVID-19 dynamics with quarantine, isolation, and environmental viral load. *Advances in Difference Equations*, 2021, 106, (2021). [CrossRef]

[15] Rezapour, S., Mohammadi, H. and Samei, M.E. SEIR epidemic model for COVID-19 transmission by Caputo derivative of fractional order. *Advances in Difference Equations*, 2020, 490, (2020). [CrossRef]

[16] Baleanu, D., Mohammadi, H. and Rezapour, S. A fractional differential equation model for the COVID-19 transmission by using the Caputo-Fabrizio derivative. *Advances in Difference Equations*, 2020, 229, (2020). [CrossRef]

[17] Huang, C., Wang, J., Chen, X. and Cao, J. Bifurcations in a fractional-order BAM neural network with four different delays. *Neural Networks*, 141, 344-354, (2021). [CrossRef]

[18] Xu, C., Mu, D., Liu, Z., Pang, Y., Liao, M. and Aouiti, C. New insight into bifurcation of fractional-order 4D neural networks incorporating two different time delays. *Communications in Nonlinear Science and Numerical Simulation*, 118, 107043, (2023). [CrossRef]

[19] Xu, C., Liu, Z., Li, P., Yan, J. and Yao, L. Bifurcation mechanism for fractional-order three-triangle multi-delayed neural networks. *Neural Processing Letters*, (2022). [CrossRef]

[20] Xu, C., Zhang, W., Aouiti, C., Liu, Z. and Yao, L. Bifurcation insight for a fractional-order stage-structured predator–prey system incorporating mixed time delays. *Mathematical Methods in the Applied Sciences*, (2023). [CrossRef]

[21] Sene, N. SIR epidemic model with Mittag-Leffer fractional derivative. *Chaos, Solitons & Fractals*, 137, 109833, (2020). [CrossRef]

[22] Omame, A., Abbas, M. and Abdel-Aty, A.H. Assessing the impact of SARS-CoV-2 infection on the dynamics of dengue and HIV via fractional derivatives. *Chaos, Solitons & Fractals*, 162,

112427, (2022). [CrossRef]

[23] Omame, A., Abbas, M. and Onyenegecha, C.P. A fractional order model for the co-interaction of COVID-19 and Hepatitis B virus. *Results in Physics*, 37, 105498, (2022). [CrossRef]

[24] Omame, A., Okuonghae, D., Nwajeri, U.K. and Onyenegecha, C.P. A fractional-order multi-vaccination model for COVID-19 with non-singular kernel. *Alexandria Engineering Journal*, 61(8), 6089-6104, (2022). [CrossRef]

[25] Omame, A., Nwajeri, U.K., Abbas, M. and Onyenegecha, C.P. A fractional order control model for Diabetes and COVID-19 co-dynamics with Mittag-Leffler function. *Alexandria Engineering Journal*, 61(10), 7619-7635, (2022). [CrossRef]

[26] Omame, A., Isah, M.E., Abbas, M., Abdel-Aty, A.H. and Onyenegecha, C.P. A fractional order model for Dual Variants of COVID-19 and HIV co-infection via Atangana-Baleanu derivative. *Alexandria Engineering Journal*, 61(12), 9715-9731, (2022). [CrossRef]

[27] Ogunrinde, R.B., Nwajeri, U.K., Fadugba, S. E., Ogunrinde, R.R. and Oshinubi, K.I. Dynamic model of COVID-19 and citizens reaction using fractional derivative. *Alexandria Engineering Journal*, 60(2), 2001-2012, (2021). [CrossRef]

[28] Atangana, A. and Secer, A. A note on fractional order derivatives and table of fractional derivatives of some special functions. *Abstract and Applied Analysis*, 2013, 279681, (2013). [CrossRef]

[29] Gorenflo, R., Mainardi, F. Fractional Calculus. In: Carpinteri, A., Mainardi, F. (eds) Fractals and Fractional Calculus in Continuum Mechanics. International Centre for Mechanical Sciences, vol 378. Springer, Vienna, (1997). [CrossRef]

[30] Liu, K., Feckan, M. and Wang, J. Hyers–Ulam stability and existence of solutions to the generalized Liouville–Caputo fractional differential equations. *Symmetry*, 12(6), 955, (2020). [CrossRef]

[31] https://www.populationpyramid.net/nigeria/2021/ (Access Date: February 2023).

[32] United States Food and Drug Administration, https://www.fda.gov/media/144245/download, (2021), (Access Date: January 2023).

[33] Nwajeri, U.K., Omame, A. and Onyenegecha, C.P. Analysis of a fractional order model for HPV and CT co-infection. *Results in Physics*, 28, 104643, (2021). [CrossRef]

[34] Diethelm, K. and Freed, A.D. The FracPECE subroutine for the numerical solution of differential equations of fractional order. *Forschung und Wissenschaftliches Rechnen*, 57-71, (1998).

[35] McCall, J. Genetic algorithm for modeling and optimization. *Journal of Computational and Applied Mathematics*, 184(1), 205-222, (2005). [CrossRef]

Bulletin of Biomathematics (BBM)
(https://bulletinbiomath.org)

How to cite this article: Atede, A.O., Omame, A. & Inyama, S.C. (2023). A fractional order vaccination model for COVID-19 incorporating environmental transmission: a case study using Nigerian data. *Bulletin of Biomathematics*, 1(1), 78-110. https://doi.org/10.59292/bulletinbiomath.2023005